ADVANCING EARTH AND SPACE SCIENCES

Tectonics

RESEARCH ARTICLE
10.1029/2023TC007828

Alpine Ductile Deformation of the Upper Iberian Collided Margin (Eaux-Chaudes Massif, West-Central Pyrenean Hinterland, France)

Norbert Caldera[1], Antonio Teixell[1], Albert Griera[1], Pierre Labaume[2], and Marc Guardia[1]

[1]Departament de Geologia, Universitat Autònoma de Barcelona, Bellaterra (Barcelona), Spain, [2]Géosciences Montpellier, Université de Montpellier, CNRS, Montpellier, France

Key Points:

- Alpine ductile deformation and nappe stacking involving basement evidence a tectonic style not reported previously for the Alpine Pyrenees
- Unusual tertiary weld-like structures have been recognized within the autochthon upper Cretaceous rocks
- Strong structural variability is evidenced along the Eaux-Chaudes massif

Supporting Information:

Supporting Information may be found in the online version of this article.

Correspondence to:

N. Caldera,
norbertcg4@gmail.com

Citation:

Caldera, N., Teixell, A., Griera, A., Labaume, P., & Guardia, M. (2023). Alpine ductile deformation of the upper Iberian collided margin (Eaux-Chaudes massif, west-central Pyrenean hinterland, France). *Tectonics*, *42*, e2023TC007828. https://doi.org/10.1029/2023TC007828

Received 6 MAR 2023
Accepted 8 OCT 2023

Author Contributions:

Conceptualization: Norbert Caldera, Antonio Teixell, Albert Griera, Pierre Labaume
Data curation: Norbert Caldera
Formal analysis: Norbert Caldera
Funding acquisition: Antonio Teixell
Investigation: Norbert Caldera, Antonio Teixell, Albert Griera, Pierre Labaume, Marc Guardia
Methodology: Norbert Caldera, Antonio Teixell, Albert Griera, Marc Guardia
Project Administration: Antonio Teixell, Albert Griera
Resources: Antonio Teixell, Albert Griera

Abstract The Eaux-Chaudes massif provides keys to unravel the deep-seated deformation of the Iberian rifted margin during the Alpine orogeny in the Pyrenees. The massif conforms to an inlier of upper Cretaceous carbonate rocks within the Paleozoic basement of the western Axial Zone, originally deposited in the upper margin shelf before the Cenozoic collision. New geological mapping and cross-section construction lead to the description of the lateral structural variation from a km-scale fold nappe in the west to a ductile, imbricate fold-thrust fan in the east. The transition from a Variscan pluton to Devonian metasediments underlying the autochthonous Cretaceous induced this structural change. Recumbent folding, which involved upper Paleozoic rocks, was facilitated by a lower detachment in Silurian slates and an upper detachment in an overlying Keuper shale and evaporite thrust sheet. Remnants of this allochthonous sheet form shale and ophite bodies pinched within the upper Cretaceous carbonates, conforming unusual tertiary welds. Ductile shear in the overturned limb of the Eaux-Chaudes fold nappe imparted strong mylonitic foliation in carbonate rocks, often accompanied by N-S stretching lineation and top-to-the-south kinematic indicators. The burial of the massif by basement-involved thrust sheets and the Keuper sheet, along with their Mesozoic-Cenozoic cover, account for ductile deformation conditions and a structural style not reported hitherto for the Alpine Pyrenees. A hypothesis for the tectonic restoration of this part of the Pyrenean hinterland is finally proposed.

1. Introduction

How did inversion tectonics occur along collided continental margins? This is a complex question that depends on the specific geodynamic history within the Wilson Cycle (e.g., Manatschal et al., 2021). During the early stages of orogeny, tectonic inversion is mainly controlled by inherited factors such as the mechanical stratigraphy of the sedimentary cover and the nature of basement structures formed during previous tectonic events (e.g., Butler et al., 2006). At upper crust levels, contractional deformation typically occurs by the reactivation of extensional faults, by the development of detachment levels following weak mechanical horizons such as salt, shale or fluid-overpressured units. In foreland fold-and-thrust belts, synorogenic sediments give key information to decipher the collision history, but in orogenic hinterlands, where polydeformed basement rocks dominate in outcrop, constraining the inversion tectonics of a particular event is challenged by the absence of unequivocal markers.

The Wilson cycle in the Pyrenees is well-documented and divided into two main stages. It commences with the Mesozoic rifting, which culminates at mid-Cretaceous times (Aptian to early Cenomanian) with hyper-extension (Jammes et al., 2009; Lagabrielle et al., 2010), and is followed by the late Cretaceous to Cenozoic orogenic stage which created the Pyrenean mountain belt. The characteristic non-cylindricity of the Pyrenean orogen has been attributed to the extensional inheritance (e.g., Chevrot et al., 2018; Manatschal et al., 2021), especially accounting for the mechanical weakening of the basement. Saspiturry et al. (2022) recently postulated crustal-scale transfer zones partitioning the western part of the Pyrenees in an ensemble of narrow segments favoring a lateral structural variation.

This paper extends the study of the km-scale ductile fold nappe presented by Caldera et al. (2021) for a section of the Eaux-Chaudes massif (ECM) of the Pyrenean hinterland (western Axial Zone), exploring now the 3D architecture and lateral structural variation along the massif. The ECM massif, which formerly constituted the upper part of the Iberian rifted margin, preserves an upper Cretaceous inlier between Paleozoic metasedimentary and

Supervision: Antonio Teixell, Albert Griera
Validation: Norbert Caldera, Antonio Teixell, Albert Griera
Visualization: Norbert Caldera, Albert Griera, Pierre Labaume, Marc Guardia
Writing – original draft: Norbert Caldera
Writing – review & editing: Antonio Teixell, Albert Griera, Pierre Labaume, Marc Guardia

igneous rocks of the Axial Zone, previously deformed by the Variscan orogeny (Ternet, 1965) (Figure 1). The objective of this work is to take advantage of the occurrence of the Cretaceous rocks to obtain clues of the Alpine deformation in the Pyrenean hinterland, where it is often blurred by the dominant basement exposure (Figure 1b).

Here, we also document a stack of upper thrust sheets, originated at the necking zone of the Iberian margin, that buried the ECM accounting for ductile deformation conditions in the collided margin (Figure 2). We, thus, address the role of the mechanical stratigraphy by discussing the role of detachment levels both in basement and cover, and of an igneous body hosted in the Paleozoic metasediments.

2. Tectonic Framework

Two orogenic episodes (Variscan and Alpine-Pyrenean) separated by two rifting stages (Permo-Triassic and late Jurassic-mid Cretaceous) have defined the structural architecture of the Pyrenees. The Variscan orogeny configured the Paleozoic basement structure between ca. 380–280 Ma (Cochelin et al., 2017, and references therein), and culminated with the intrusion of granitic plutons around 300 Ma. The Permo-Triassic extension is recorded by terrestrial red beds, starting in the study area with siliciclastic sandstones and conglomerates of the Lower Triassic Buntsandstein facies. In the Pyrenean domain, the Buntsandstein is overlain by red-green claystones and salt of Keuper facies (Biteau et al., 2006; Ortí et al., 2017), containing Muschelkalk marine limestone intercalations (Stevaux & Winnock, 1974). The Keuper facies host abundant subvolcanic bodies of dolerites ("ophites"). The main rifting in the Pyrenees occurred during early and mid-Cretaceous times inducing a strong crustal stretching (Espurt et al., 2019; Grool et al., 2018; Jammes et al., 2009; Lagabrielle & Bodinier, 2008; Lagabrielle et al., 2010; Manatschal et al., 2021; Masini et al., 2014; Mouthereau et al., 2014; Teixell et al., 2016; Tugend et al., 2014). As a result, the mantle was exhumed between the Iberian and Eurasian rifted margins with maximum basin subsidence in the Albian-early Cenomanian, when the Mendibelza conglomerates accumulated in the necking zone of the Iberian margin and deeper water flysch in the distal margin (Souquet et al., 1985). Pre- and syn-rift sediments where locally affected by High Temperature-Low Pressure metamorphism (e.g., Clerc et al., 2015; Clerc & Lagabrielle, 2014; Ducoux et al., 2021; Golberg, 1987; Golberg & Leyreloup, 1990; Lagabrielle et al., 2010). Salt tectonics Keuper evaporites developed from the early Cretaceous (e.g., Labaume & Teixell, 2020, and references therein).

Within the Cretaceous rift, a transition from syn- to post-rift sedimentation is ascribed to the mid-Cenomanian, recorded by a regional-scale unconformity (e.g., Debroas, 1987, 1990) on which expansive late Cenomanian deposits overlap the basement and lower Triassic rocks of the rift shoulders. During the Late Cretaceous, shallow platform carbonates ("Calcaires des Cañons"; Fournier, 1905) were widely developed in both the Iberian and the European upper margins, while the former rift axis still accumulated turbidite deposits (e.g., Cuvillier et al., 1964; Floquet et al., 1988; Puigdefàbregas & Souquet, 1986; Razin, 1989). Today these shelf carbonates constitute the bulk of the ECM, where they overlie Devonian metasediments and the late Carboniferous Eaux-Chaudes granite pluton (Debon, 1976, 1996; Izquierdo-Llavall et al., 2012; Ternet et al., 2004).

The Pyrenean orogeny took place from the late Santonian (ca. 84 Ma) to the early Miocene (ca. 20 Ma) (e.g., Cruset et al., 2020; Ford et al., 2022; Grool et al., 2018; Labaume et al., 2016; Muñoz, 1992, and references therein). It caused: (a) the inversion of rift-axis, including the shortening of previous salt diapirs, and the flexure-driven drowning of the post-rift platforms initiating synorogenic flysch deposition, and (b) the collision of the margins, which led to the subduction of the Iberian lower crust and the development of a south-verging, basement-involved thrust stack in the Iberian upper crust (Muñoz, 1992; Teixell et al., 2018). The ECM and overlying thrust sheets, now in the Pyrenean hinterland of the northern Axial Zone, uniquely record the compressional deformation of the Iberian margin, from the shelf to the exhumed mantle domain.

3. Structural and Stratigraphic Domains in the Study Area

The stratigraphic succession of the ECM is well-constrained (Ternet et al., 2004). In what follows, we first describe the stratigraphy (Figure 3), and then the broad tectonic configuration of the study area, which consists of five main tectono-sedimentary domains (Figure 4) arranged from bottom to top as: (a) the Gavarnie nappe with upper Cretaceous carbonate rocks unconformable on Paleozoic metasediments and granite, with scarce Buntsandstein remnants in between (Figure 2) and (b) the Eaux-Chaudes nappe (ECN), with allochthonous upper Cretaceous

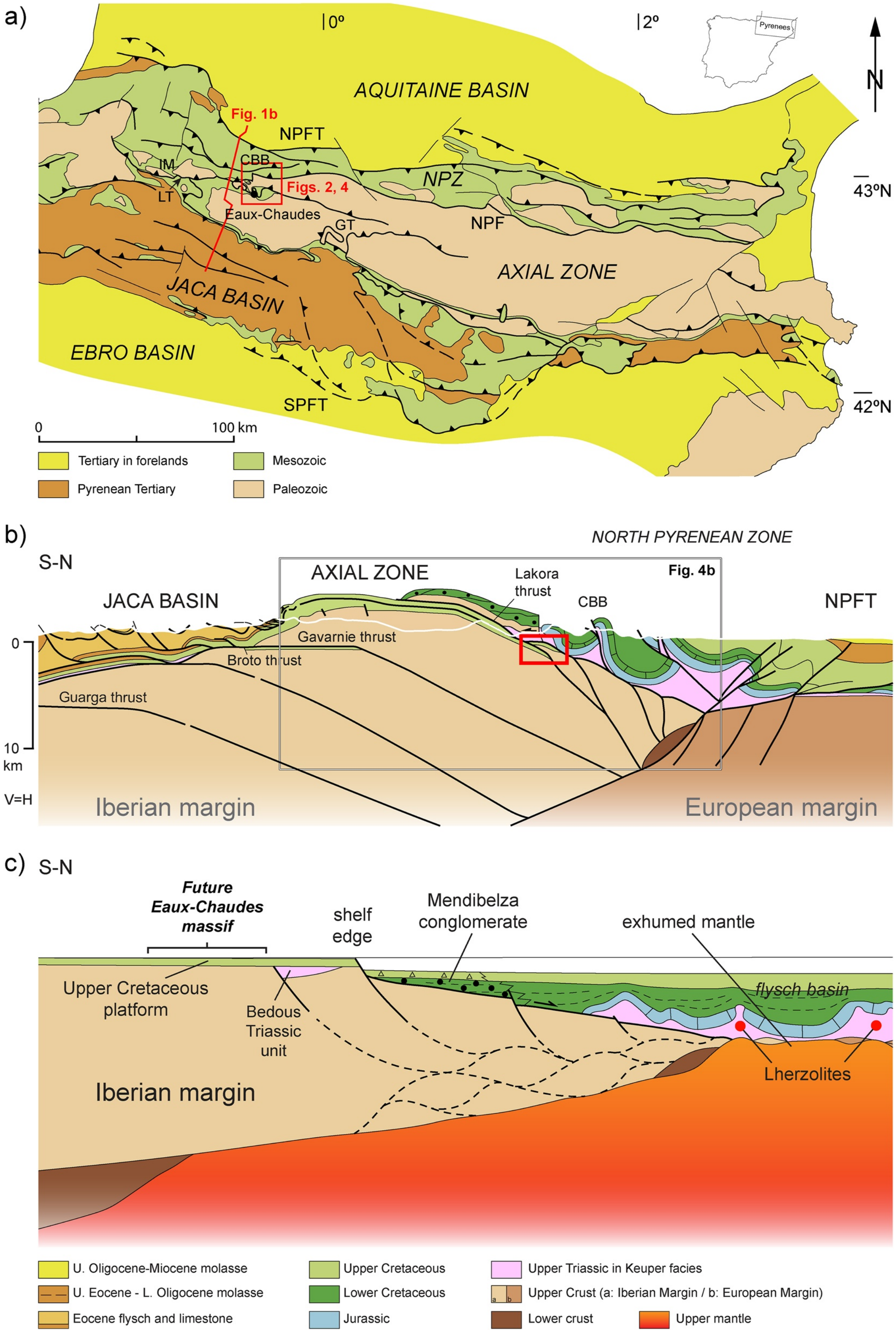
a)
0º
2º
Pyrenees
N
AQUITAINE BASIN
Fig. 1b
NPFT
CBB
IM
LT
Figs. 2, 4
NPZ
43ºN
Eaux-Chaudes
GT
NPF
AXIAL ZONE
JACA BASIN
EBRO BASIN
SPFT
42ºN
0
100 km
Tertiary in forelands
Mesozoic
Pyrenean Tertiary
Paleozoic
b)
NORTH PYRENEAN ZONE
S-N
AXIAL ZONE
Lakora thrust
Fig. 4b
JACA BASIN
CBB
NPFT
0
Gavarnie thrust
Broto thrust
Guarga thrust
10 km
V=H
Iberian margin
European margin
c) S-N
Future Eaux-Chaudes massif
shelf edge
Mendibelza conglomerate
exhumed mantle
Upper Cretaceous platform
Bedous Triassic unit
flysch basin
Lherzolites
Iberian margin
U. Oligocene-Miocene molasse
U. Eocene - L. Oligocene molasse
Eocene flysch and limestone
Upper Cretaceous
Lower Cretaceous
Jurassic
Upper Triassic in Keuper facies
Upper Crust (a: Iberian Margin / b: European Margin)
Lower crust
Upper mantle

Figure 1.

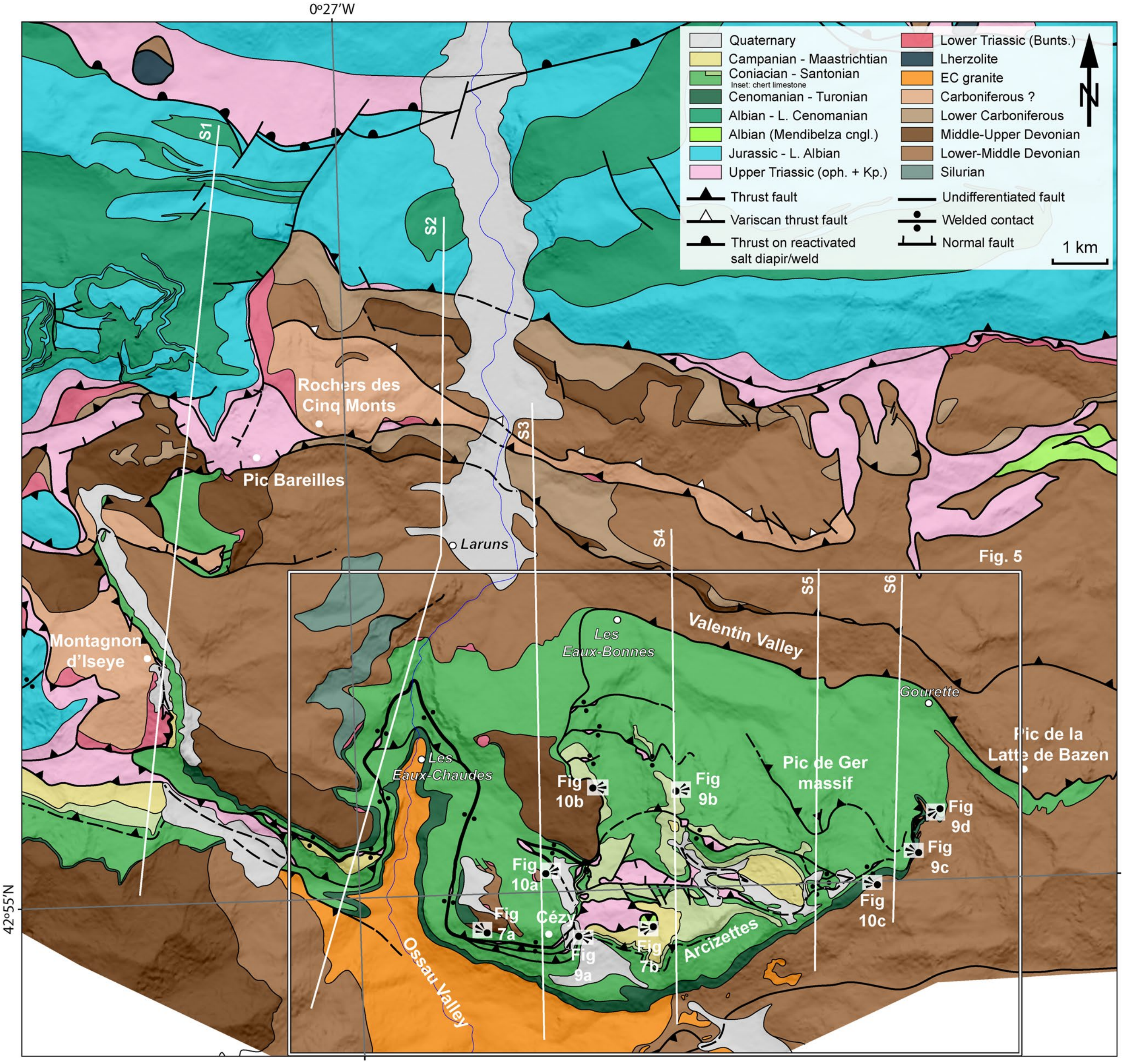

Figure 2. Geological map of the Eaux-Chaudes massif and surrounding areas (location in Figure 1a). Data compiled from published maps (Caldera et al., 2021; Labaume & Teixell, 2020; Ternet, 1965; Ternet et al., 2004), and own field observations. White frame indicates the mapped area amplified in Figure 5. S1–S3: cross-sections in Figure 6. S4–S6: cross-sections in Figure 8. Indicated in the legend with a question mark is an azoic succession of limestones and slates attributed tentatively to the Carboniferous by Ternet et al. (2004) and labeled hCM in Figure 3.

carbonates and Paleozoic metasediments involved in complex folding. (c) the Paleozoic-bearing thrust sheets overlying the ECM, comprising metasedimentary basement rocks with local Buntsandstein pods and Keuper, (d) the assemblage of allochthonous Keuper rocks of the Bedous unit, overlying all the units described above (Figure 1c), and finally (d) the Chaînons Béarnais Belt (CBB) of the North Pyrenean Zone (NPZ) consisting

Figure 1. (a) Geologic sketch map of the Pyrenees showing the location of the Eaux-Chaudes massif. Red frame indicates the mapped area (Figures 2 and 4) and red line indicates cross-section in Figure 1b. (b) Crustal cross-section of the Pyrenees west of the study area (simplified from Teixell et al., 2016) showing the tectonic setting of the Eaux-Chaudes structures (red frame). Black frame indicates the part of the section used to show the Lakora thrust system trace in Figure 4b. (c) Restored crustal cross-section of the Iberian margin and rift axis to the Late Cretaceous (Santonian) from Figure 1b (modified from Teixell et al., 2016). CBB, Chaînons Béarnais Belt; IM, Iguntze and Mendibelza massifs; GT, Gavarnie thrust; LT, Lakora thrust; NPZ, North Pyrenean Zone; NPF, North Pyrenean Fault; NPFT, North Pyrenean Frontal thrust; SPFT, South Pyrenean Frontal thrust.

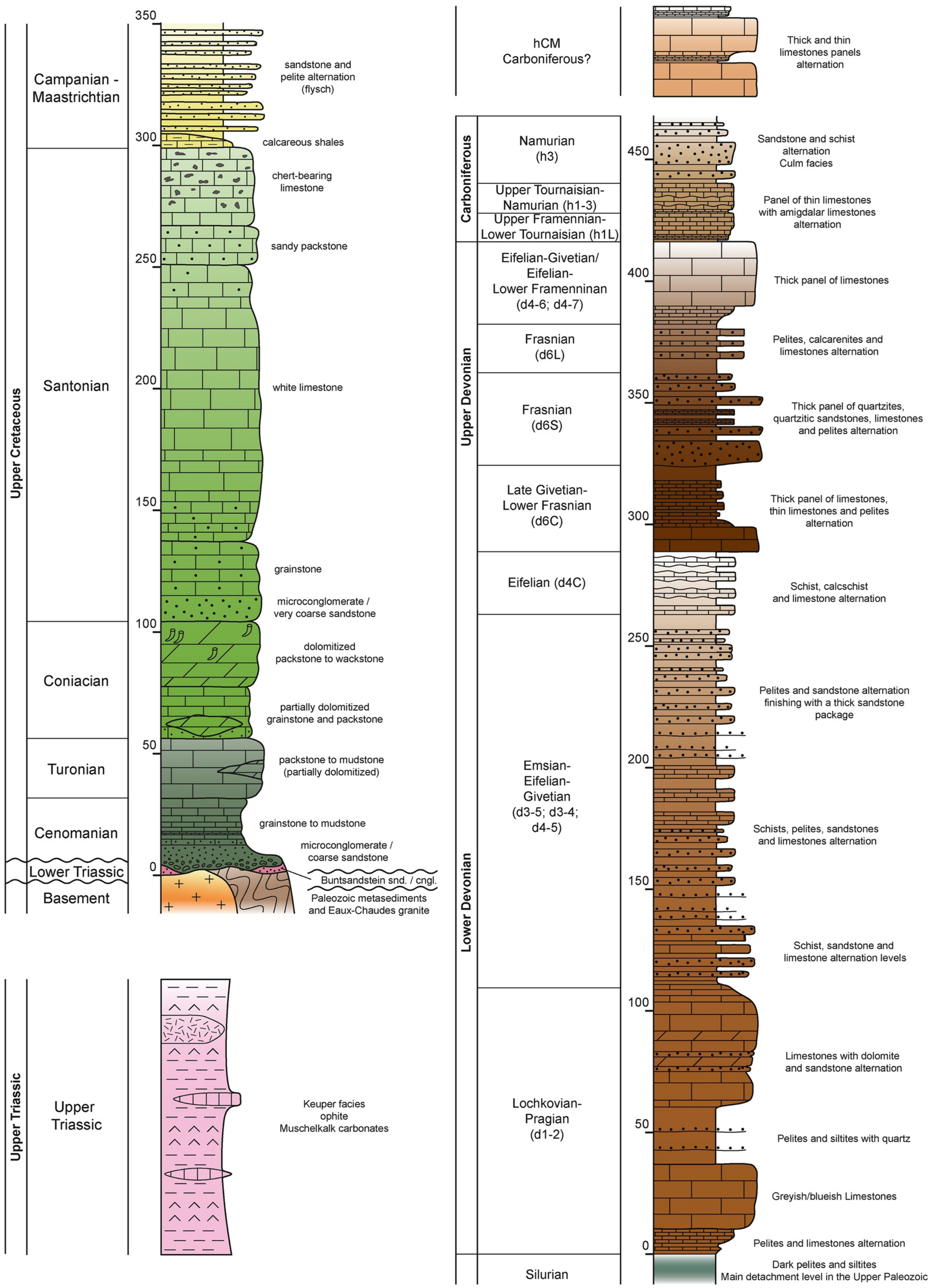

Figure 3. Simplified stratigraphic logs of the Paleozoic and Mesozoic of the Eaux-Chaudes massif (based on Ternet, 1965, and own data).

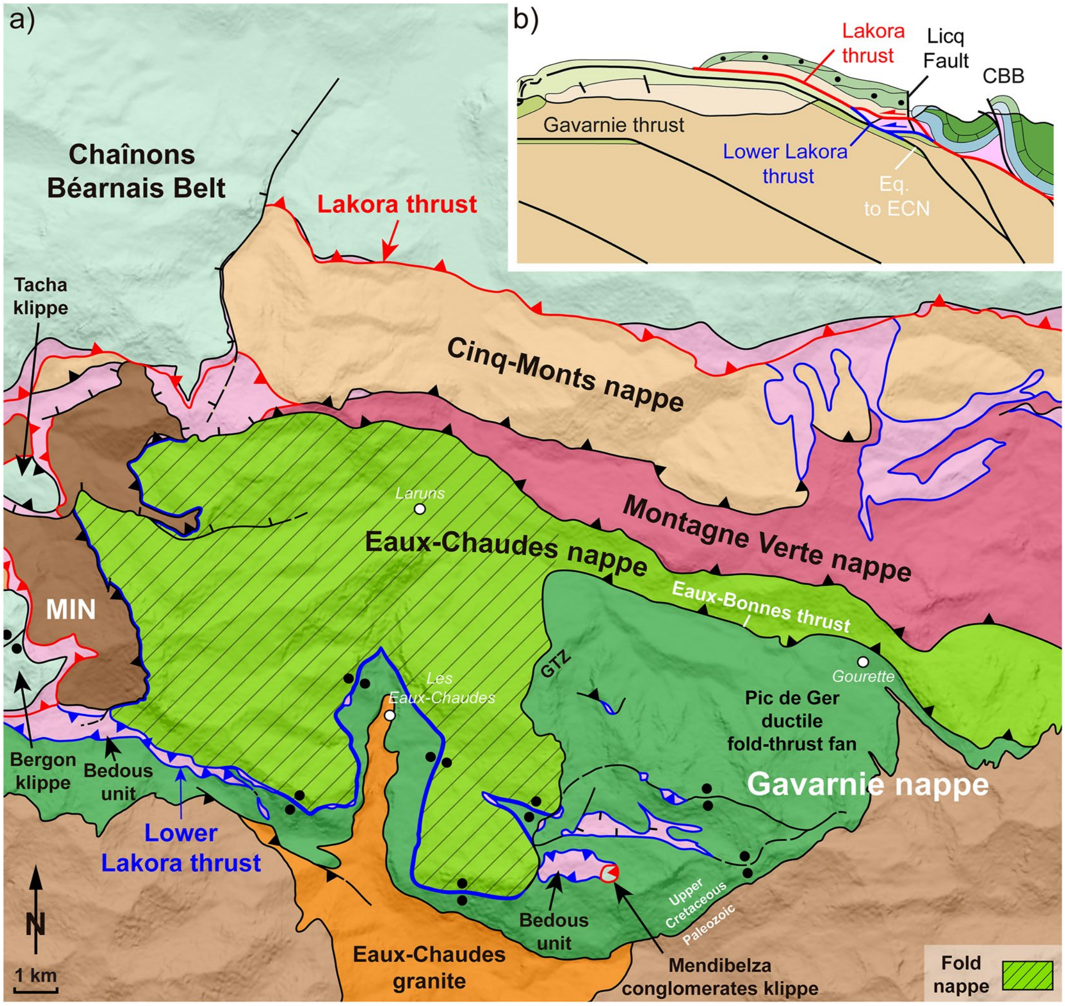

Figure 4. (a) Simplified tectonic map of the Eaux-Chaudes massif and southern edge of the Chaînons Béarnais Belt showing the structural units referred to in the text. Bedous unit corresponds to the upper Triassic carried by the Lower Lakora thrust. MIN, Montagnon d'Iseye nappe; GTZ, Gourzy Transfer Zone. (b) Detail of the cross-section in Figure 1b of the Gavarnie nappe and overlying tectonic units indicating the structural position of the Lower Lakora thrust and Lakora thrust *s.s.*

of a thick Jurassic and Lower Cretaceous carbonate and shale succession detached on the Triassic Keuper. This last succession is affected by low-grade thermal metamorphism acquired during the Cretaceous rifting.

3.1. Stratigraphy of the Eaux-Chaudes Massif and Surroundings

3.1.1. Paleozoic Basement and Lower Triassic

The pre-Mesozoic basement around the ECM consists of upper Paleozoic low-grade metasedimentary rocks (Figure 3). The oldest unit in the area corresponds to Silurian black slates (Mirouse, 1962), with interbedded thin limestone layers. It is considered as the main regional detachment level for the Paleozoic of the Axial Zone (e.g., García-Sansegundo et al., 2011, and references therein). Above this unit, an approximately 400–500 m thick succession of interlayered pelites, limestones, sandstones and quartzites of Devonian age is observed, followed by a few hundred meters thick succession of clastic turbidites and limestones of Carboniferous age (Culm facies; Delvolvé, 1987). These rocks host the Eaux-Chaudes granitic pluton, which is late Carboniferous in age (301 ± 9, Guerrot, 2001) (Figure 2). In some thrust sheets overlying the ECM, an azoic succession of limestones and schists, with local sandstone layers, is tentatively attributed to the Carboniferous (Ternet et al., 2004; Labeled hCM in Figure 3).

Discontinuous lower Triassic conglomerate and sandstone deposits (Buntsandstein facies) rest unconformably over the Paleozoic basement. In the ECM and overlying thrust units, pre-late Cretaceous erosion removed a vast volume of Buntsandstein, but some pods have been preserved. They form useful markers to constrain boundaries of stratigraphic nature and polarity relationships between the upper Cretaceous and Devonian limestones of the ECM.

3.1.2. Allochthonous Triassic Sheet

The middle-upper Triassic Keuper of the Bedous unit (Figure 3) consists of a melange of claystones, cargneules, Muschelkalk limestones, and ophites (Ternet, 1965; Ternet et al., 2004). Salt is not observed at the surface but is well documented nearby in the subsurface in adjacent basins of the northern Pyrenees (e.g., Biteau et al., 2006; Ortí et al., 2017; Soto et al., 2017). It should be emphasized that the Keuper is not found along the main unconformity between the Paleozoic basement and the upper Cretaceous carbonates of the ECM but it forms an allochthonous thrust sheet emplaced over the upper Cretaceous (e.g., Caldera et al., 2021; Canérot et al., 2004; Figures 2 and 4).

3.1.3. Upper Cretaceous

The Cretaceous stratigraphy of the ECM has been thoroughly investigated in previous works (e.g., Alhamawi, 1992; Casteras, 1956; Casteras & Souquet, 1964; Ternet, 1965). It is characterized by a post-rift carbonate platform succession (from Cenomanian to Santonian) followed by syn-orogenic shale and flysch deposits (Campanian-Maastrichtian) (Figure 3).

At the base of the upper Cretaceous, the Cenomanian with a maximum thickness of ca. 25 m, unconformably lies on the Paleozoic basement or the Buntsandstein. Occasionally, it begins with a quartz-rich microconglomerate or coarse-grained sandstone, followed by a succession of grainstones to mudstones with *Praealveolina* and *Pseudocyclammina*. The transition to the Turonian is highlighted by packstone to mudstone deposits featuring a *Chrysalidina* and *Nezzazata* fossil content. Debris of echinoderms, *Pithonella*, *Halimeda ellioti* and *Globotrunca helvetica bolli* are also characteristic of this unit (Conard & Rioult, 1977). The Turonian limestone shows a varying thickness, with a maximum of 80 m (Alhamawi, 1992). The Coniacian corresponds to partially dolomitized grainstones and packstones with a maximum thickness of ca. 40 m (Ternet et al., 2004), and dominated at the base by debris of *Hippurites* rudists, polypers, gasteropods and foraminifera. To the top, there are packstones to wackestones with benthic foraminifera, rudists, oysters, and polypers. In the southern flank of the Arcizettes Mountains (Figure 2), this unit is largely dolomitized.

The Santonian is a massive white limestone unit, with a thickness of ca. 250 m (Ternet, 1965), forming the tallest reliefs of the ECM. It begins with microconglomerate or coarse sandstone cemented by calcite and containing rounded quartz grains. The white limestone contains decimetric levels of slightly sandy packstones with high content of *Lacazina* and bivalve debris. The top of the Santonian is characterized by a 6–30 m layer of limestone with chert nodules, a characteristic key level in the western Axial Zone (Souquet, 1967; Teixell et al., 2000) (Figure 2). The top of the upper Cretaceous sedimentary record of the ECM is composed of an alternation of pelites and sandstones up to several hundred meters thick referred to as the Campanian flysch (Ternet et al., 2004). Sandstones show grain-size gradation and cross-stratification with quartz grains and white-mica slats, with mainly benthic microfauna in the sandstones (e.g., *Orbitoides media*, *Orbitoides tissoti*, *Nummofallotia cretacea*), and pelagic microfauna in the pelites (e.g., *Globotruncata elevata*, *Globotruncata rosetta*) (Ternet et al., 2004). At the base of this unit we can locally observe a 10 to 15 m-thick level of calcareous shales.

The upper Cretaceous limestones represent the post-rift shelf in the upper Iberian margin. The transition from the platform limestones to the shales and flysch-type sediments of the uppermost Cretaceous mark an abrupt deepening of the margin attributed to foreland flexure in the early steps of the Pyrenean orogeny (Labaume et al., 2016; Teixell, 1996).

3.2. Structural Units

3.2.1. The Gavarnie and Eaux-Chaudes Nappes

A summary of all the acronyms used for the structural units in the following is provided in table 1. As introduced above, the Gavarnie and Eaux-Chaudes nappes are made of upper Cretaceous carbonates unconformably lying on the Paleozoic basement. The ECN includes the Eaux-Chaudes fold nappe (ECFN), observable on both

Table 1
Table of Acronyms Used for Large-Scale Structures of the Study Area

Acronym	Referred unit
ECFN	Eaux-Chaudes Fold Nappe
ECN	Eaux-Chaudes Nappe
ECM	Eaux-Chaudes Massif
MIN	Montagnon d'Iseye Nappe
5MN	Cinq-Monts Nappe
MVN	Montagne Verte Nappe
CBB	Chaînons Béarnais Belt
EBT	Eaux-Bonnes Thrust
LT	Lakora Thrust
LwLT	Lower Lakora Thrust

sides of the Ossau Valley (Figures 4 and 5; Caldera et al., 2021). This fold involves the upper Cretaceous carbonates and the upper Paleozoic succession that occupies the fold core. The recumbent limb directly rests above the relative autochthonous upper Cretaceous carbonates of the Gavarnie nappe. Large-scale recumbent folds have not been previously reported in the context of the Alpine Pyrenees but are documented in the Paleozoic basement where they are attributed to the Variscan orogeny (Aerden & Malavieille, 1999; Matte, 2002, and references therein; Bastida et al., 2014). Carbonates from the overturned limb attest for strong ductile deformation while the normal limb and the autochthon are little-deformed, preserving sedimentary textures and fossil content, and featuring a spaced pressure-solution cleavage (Caldera et al., 2021). The autochthonous upper Cretaceous carbonates continue to the west as a north-dipping monocline and then as a large antiformal fold around the western termination of the Axial Zone (Figures 1a and 1b).

To the east, in the Valentin valley, the upper Cretaceous of the ECN has been eroded and the unit comprises only Devonian sediments in the hanging-wall of the Eaux-Bonnes thrust (Bresson, 1903). In this area, it overrides the upper Cretaceous carbonates of the Gavarnie nappe affected by ductile deformation in the Pic de Ger fold-thrust fan (Figure 2, GTZ in Figures 4 and 5). The transition between the little-deformed autochthon, in the west, to the fold-thrust fan, in the east, occurs through a relatively narrow transfer zone, here named the Gourzy transfer zone, located between the Pic du Gourzy and Montcouges, and passing by Les Eaux-Bonnes village to the north (Figures 2, 4, and 5). This transfer zone consists of a high-angle west-dipping tear fault system, which causes a recess of the ECN, passing from the far-reaching recumbent fold nappe to the west to the Devonian in the hanging wall of the Eaux-Bonnes thrust to the east. The Pic de Ger ductile fold-thrust system is envisaged to partly take over the shortening of the ECFN to the east.

3.2.2. The Paleozoic-Bearing Thrust Sheets Above the Eaux-Chaudes Fold Nappe

The ECFN is overlain by a stack of basement-involved thrust sheets (Figure 4), first reported by Majesté-Menjoulas (1968) and later mapped by Ternet et al. (2004). The first unit overlying the ECFN is the Montagnon d'Iseye fold nappe (MIN), located on the western edge of the massif (Caldera et al., 2021; Labaume & Teixell, 2020). We observed that the structure of the MIN corresponds in the southern part to a south-verging recumbent fold with a ~2 km-long overturned limb outlined by the Triassic Buntsandstein and cored by Carboniferous rocks, while in the northern part it comprises Devonian and Carboniferous metasediments. Late normal faults, trending E-W and dipping to the north, cut both the MIN and the Cretaceous and Paleozoic core of the underlying ECFN (Figure 2). The second overlying unit corresponds to the Montagne Verte nappe (MVN) (Figure 4), formed by upper Devonian to Lower Carboniferous metasediments. This unit thins cartographically from ~3.5 km wide in the eastern limit of the study area and disappears westward where it is separated from the MIN by the Keuper of the Pic de Bareilles area (Figure 4). No overturned limb was identified in this unit. The uppermost basement-involved unit is the Cinq-Monts nappe (5MN) (Figure 4), composed of Devonian and Carboniferous rocks and also containing an overturned Buntsandstein limb at its front. The 5MN features an internal thrust fault mapped by Ternet et al. (2004) and sealed by the Buntsandstein, which can be thus attributed to the Variscan orogeny (Figure 2).

3.2.3. The Lakora Thrust System and the Chaînons Béarnais Belt

The ECM and the Paleozoic-bearing thrust sheets are overlain by the Lakora thrust system (red and blue lines in Figure 4). The Lakora thrust system is related to the inversion of the Iberian rifted margin since the latest Cretaceous (Teixell, 1993; Teixell et al., 2016). In the study area the Lakora thrust *s.s.* (as defined by Teixell, 1993) carries the Jurassic-Lower Cretaceous sedimentary rocks of the CBB, a segment of the NPZ to the south (red line in Figure 4). At its base, it occurs a thick Keuper thrust horse (the Bedous Triassic sheet of Labaume & Teixell, 2020) (Figure 4), whose sole thrust is here referred to as the Lower Lakora thrust (LwLT; blue lines in Figure 4). The CBB is a salt-detached fold-and-thrust system made of Triassic Keuper to lower Cretaceous rocks (carbonates, shales and flysch) from the former rift axis, affected by diapiric structures and containing mantle (lherzolite) lenses (Labaume & Teixell, 2020). Two southern outliers of the CBB are preserved above the western termination of the Montagnon d'Iseye nappe (MIN): the Tacha and Bergon klippes (Figures 2 and 4a). The

10.1029/2023TC007828

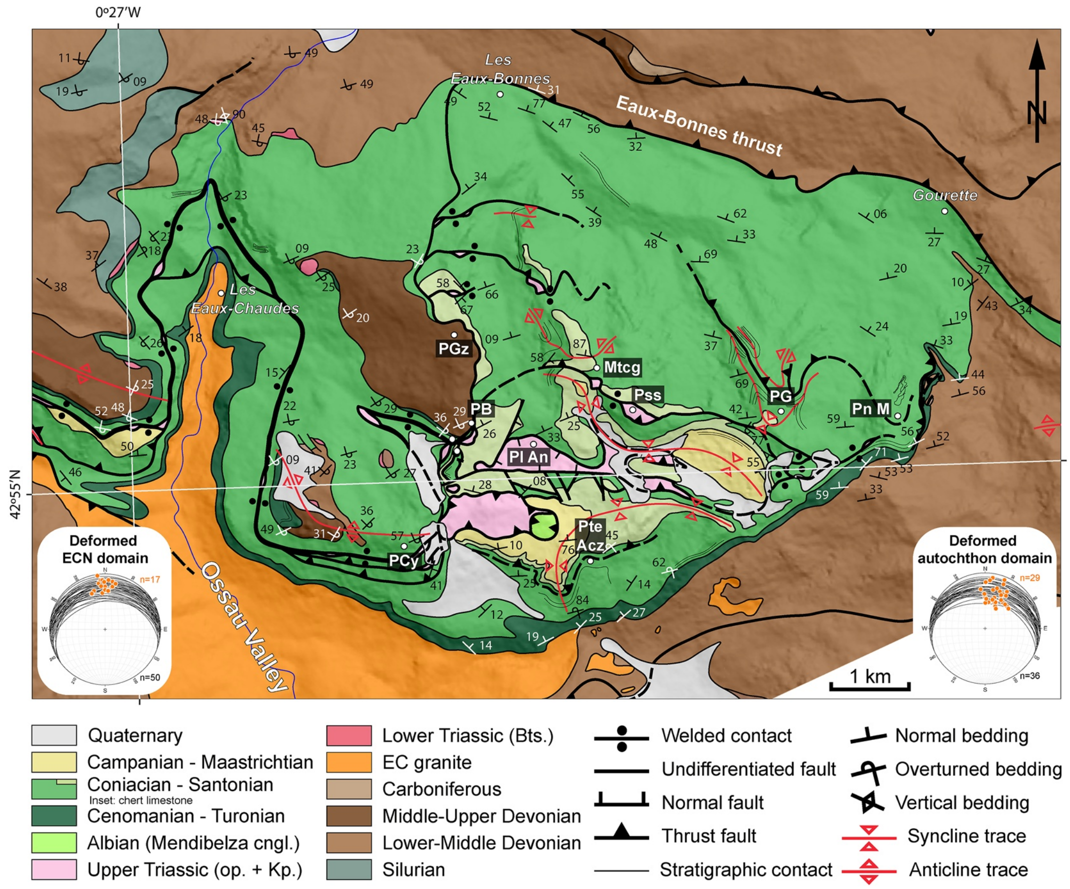

Figure 5. Detailed geological map of the Eaux-Chaudes massif (from Figure 2) showing structural data and the situation of the main localities referred to in the text. In the lower corners we show projections of cleavage (black lines) and stretching lineation (orange points) of ductily deformed upper Cretaceous rocks from the Eaux-Chaudes nappe (left) and the Pic de Ger fold-thrust fan (right). PCy, Pic de Cézy; PGz, Pic du Gourzy; PB, Pic de Brèque; Pl An, Plateau d'Anouilhas; Pte Acz, Petite Arcizette; Mtcg, Montcouges; Pss, Pambassibé; PG, Pic de Ger; Pn M, Pêne Médaa.

allochthony of these units over the MIN is supported by the truncation relationships of the rocks above, and by the paleotemperature contrast between the Tacha and Bergon klippes and the Triassic of the MIN (393 and 354°C, respectively; Corre, 2017). A small, isolated remnant of siliciclastic conglomerates attributed to the Albian Mendibelza formation (Ternet, 1965), characteristic of the Lakora thrust sheet to the west of the Axial Zone and originally deposited on the margin's necking zone, has been preserved over the Triassic Keuper or directly on the upper Cretaceous of the Gavarnie nappe (Figures 2, 4, and 5). In the Iguntze massif to the west, the Mendibelza conglomerate onlaps a shortcut of Paleozoic rocks and it is located south of the CBB from which it is separated by the Licq fault (Labaume & Teixell, 2020; Teixell, 1993) (Figure 3b). In the study area, the Paleozoic basement of the Mendibelza conglomerate is lacking and the relationships with the CBB (Licq Fault) have been eroded.

4. Structural Sections of the Eaux-Chaudes Massif

To describe the structure of the ECM and its lateral variation, we present six new cross-sections (Figures 6 and 8) and several interpreted outcrop images or panoramas (Figures 7 and 9). The sections are oriented approximately N-S, perpendicular to the dominant structural trend (main folds, thrusts, and foliation), and parallel to the stretching lineation (Figure 5). They have been constructed from original fieldwork with mapping revision and structural data acquisition, focused on clarifying the specific key points (e.g., bedding polarity, strain intensity), and complemented by additional data from the literature (e.g., Caldera et al., 2021; Labaume & Teixell, 2020; Ternet, 1965; Ternet et al., 2004). The Field Move and Move softwares (Petroleum Experts) were used for data acquisition and managing. Move was also used to construct the 2D section profiles (Figure S1), assisted by 3D building of stratigraphic and fault surfaces. Dip-data, stratigraphic and tectonic boundaries were projected onto a digital elevation model with a resolution of 30 × 30 m/pixel, and from this were projected on each cross-section from 1.5 km wide swaths.

3D perspectives of the cross-section series and of geological surfaces are provided as Supporting Information (Figures S1 and S2). The 3D surface model was constructed from the sections by the triangular surfaces interpolation method. Representative meshes included the top upper Cretaceous, the top of basement. This model provided feed-backs on the section elaboration process.

The description of the sections is divided into two parts to account for the different structural characteristics between the western and eastern sectors (Figure 2). While in the western sector (Ossau Valley), the structure of the ECM is dominated by the large-scale allochthonous fold nappe (the ECFN) (Figures 4 and 6), in the eastern sector (Pic de Ger massif) the structure is characterized by an imbricate fold-thrust fan in the upper Cretaceous of the Gavarnie nappe (Figure 8).

4.1. Western Sector (Ossau Valley): The Eaux-Chaudes Fold Nappe

The general structure of the ECM has been classically interpreted as a duplex with a roof thrust carrying Paleozoic rocks over the upper Cretaceous (Cochelin et al., 2017; Déramond et al., 1985; Dumont et al., 2015; Ternet, 1965). Only a short, overturned fold limb was reported by Ternet (1965) in the front of the structure without continuity to the north. Recently, the structure of this western sector has been reinterpreted as a km-scale, south-vergent recumbent fold nappe with a large, overturned limb (Caldera et al., 2021) (Figure 6). The Eaux-Chaudes section (S2 in Figure 6) has been improved from the one presented in Caldera et al. (2021). In this contribution, we further document the structure by enlarging the analyzed area and providing new structural data and field images (Figures 2, 5, and 7). Due to a general westward plunge, constraints for the upper thrust sheets are stronger to the west, while in the eastern sections, the structures projected above topography have larger uncertainties.

The autochthonous upper Cretaceous (i.e., the Mesozoic cover of the Gavarnie nappe, Figures 2 and 5) lies unconformably on the Eaux-Chaudes granite and remains weakly deformed along this sector. In the ECFN, the upper Cretaceous succession is not always complete, but it is locally preserved up to the Campanian flysch (i.e., below the Montagnon d'Iseye thrust in S1). The normal limb is weakly deformed while features observed in the upper Cretaceous carbonates of the overturned limb indicate top to the south shearing, developed under ductile conditions and moderate temperatures (315 to 328°C in the normal limb; 334 to 355°C in the overturned limb and autochthonous with an estimated geothermal gradient of 30°C/km; Caldera et al., 2021). Examples of this ductility at large and small scales are evidenced by bedding-parallel mylonitic foliation, mineral stretching lineation, S-C composite fabrics and other asymmetric kinematic indicators (i.e., calcite crystal-shape fabrics, dolomite porphyroclasts).

The fold nappe plunges to the west following the general trend of the western Axial Zone. Although there exist some small differences in the fold shape across the three sections (Figure 6), the overall geometry is consistent. The overturned stratigraphy is constrained by the presence of Buntsandstein pods, which show way-up criteria (crossbedding, grain-size grading) indicating a reverse polarity (Caldera et al., 2021), along the contact between Paleozoic and upper Cretaceous. It is worth mentioning the thinning of the upper Cretaceous in the overturned limb eastwards from Section 1 to Section 3 (Figure 6).

The hinge zone of the recumbent fold is box-shaped featuring ductile deformation in the Cretaceous rocks evidenced by stretched fossils and grain recrystallization observable in thin sections (Figure S3 in Supporting Information S1), while these rocks remained weakly deformed in the normal limb. The normal limb can be traced northwards over 5 km in the eastern slopes of the Montagnon d'Iseye and south of Pic Bareilles, where we observed its footwall cut-off under allochthonous Paleozoic (Figure 2). It must be noted that, due to the general plunge to the west, the upper Cretaceous of the Axial Zone cover is never exposed to the surface again in the western Axial Zone region. The thrust faulted syncline of the ECFN is linked in depth and eastwards with the Eaux-Bonnes thrust (e.g., Bresson, 1903; Ternet et al., 2004), well-traced in the Valentin valley ("accident du Valentin" in Ternet, 1965) (Figure 2). Several Keuper and ophite bodies remain trapped in between the overturned limb of the ECFN and the autochthon (Figures 2 and 5 and Figure S4 in Supporting Information S1), which are remnants of the allochthonous Keuper sheet (Bedous unit of the overlying lower Lakora thrust sheet) pinched in

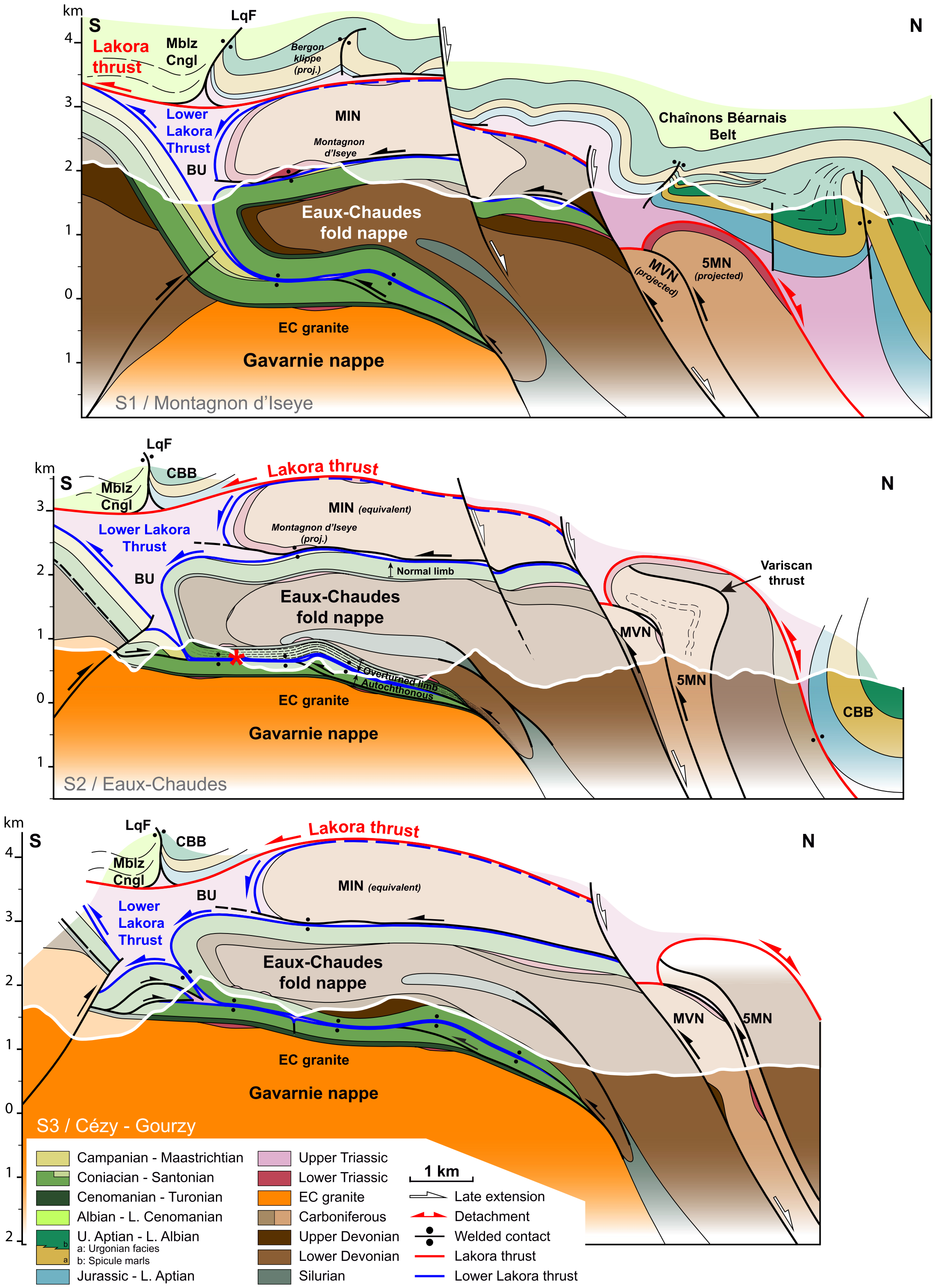

Figure 6. Geological cross-sections of the western sector of the Eaux-Chaudes massif presenting the lateral variation of the Eaux-Chaudes unit from west to east (S1–S3). See location in Figure 2. Red asterisk in S2 shows the location of the allochthon Keuper pinched in the welded syncline of the recumbent fold, shown in Sup. 1. Mblz Cngl, Mendibelza Conglomerates; LqF, Licq Fault; MIN, Montagnon d'Iseye nappe; 5MN, Cinq Monts nappe; MVN, Montagne Verte nappe; CBB, Chaînons Béarnais Belt; BU, Bedous Unit (carried by the Lower Lakora thrust). Jurassic and Lower Cretaceous rocks of the Chaînons Béarnais Belt in Section 1 are based on Labaume and Teixell (2020).

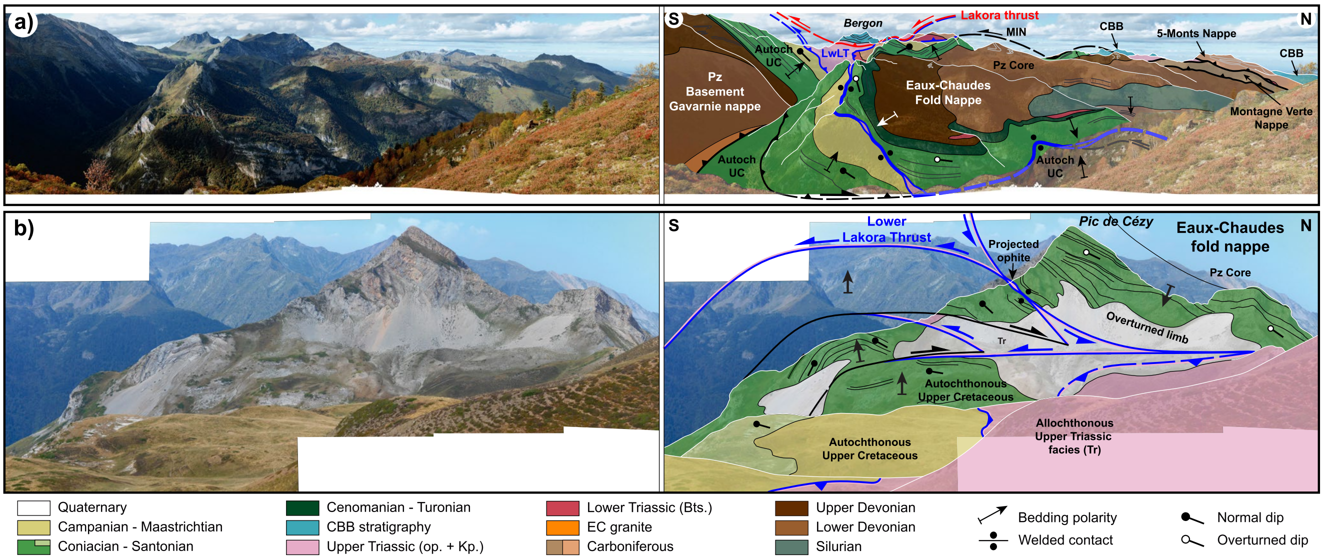

Figure 7. Interpreted panoramas showing different examples of deformation in the upper Cretaceous of the western part of the Eaux-Chaudes massif (location of views in Figure 2). (a) Interpreted panorama of the Eaux-Chaudes recumbent fold and overlying tectonic units (Montagnon d'Iseye fold nappe, Lower Lakora and Lakora thrusts, 5MN, Chaînons Béarnais Belt [CBB], Montagne Verte nappe; for explanation of acronyms, refer to the legend of the previous figure) in the Ossau Valley from an eastern viewpoint. It corresponds to the southern part of Sections 1 and 2 (Figure 6). (b) Interpreted panorama of the Pic de Cézy from an eastern viewpoint. It corresponds to the southern termination of the recumbent fold in Section 3 (Figure 6). The system of late backthrusts (black) overprints the Lower Lakora thrust (blue), which is marked by Keuper and ophite bodies.

the synformal zone between both limbs (i.e., a tertiary weld *sensu* Jackson & Hudec, 2017; Caldera et al., 2021). In the Paleozoic core of the fold, inherited Variscan folds can be recognized from stratigraphic features (light gray lines in Figure 7a and superimposed folds interpreted from an outcrop image in Figure S5 in Supporting Information S1).

South of the recumbent fold hinge, the autochthonous upper Cretaceous features small steep north-vergent back-thrusts (Caldera et al., 2021) (Figures 6 and 7), associated with the northward tilting of the northern Axial Zone. These thrusts are visible in the western side of the Ossau Valley, where they offset the Paleozoic basement and the upper Cretaceous alike (section S1 in Figures 6 and 7a; Caldera et al., 2021). The number of these north-vergent structures increases from west to east, evolving from a simple back-thrust (S1) to a small antiformal stack (section S3 in Figures 6 and 7b). On the eastern side of the Ossau Valley, on the southern slopes of the Pic du Cézy, they cause repetitions of the upper Cretaceous and Keuper (Sections S2 and S3 in Figures 6 and 7b). Ophite bodies are also pinched between the hinge of the ECFN and the imbricate sheets.

The Paleozoic stratigraphy involved in the ECFN follows the large anticlinal geometry, but inherited Variscan deformation results in a complex superimposed folding (Figure S5 in Supporting Information S1). Silurian slates form the fold core but they are locally directly in contact with the overturned upper Cretaceous (see S2 section), and to the north, they are pinched by the Devonian limestones accommodating top-to-the-south shearing.

Over the ECFN, we have represented the Paleozoic-bearing upper thrust sheets (i.e., the Montagnon d'Iseye, Montagne Verte and Cinq Monts nappes). Frequent Keuper pods are pinched between the thrust units, derived from the overlying lower Lakora thrust sheet. The bulk of the Lakora thrust unit carries the whole stratigraphy of the CBB together with Mendibelza conglomerate inliers (e.g., Figures 4, 6, and 8), which we interpret separated by the Licq fault as is observed more to the west (Labaume & Teixell, 2020; Teixell, 1993).

4.2. Eastern Sector (Pic de Ger Massif): The Ductile Fold-Thrust System

Cross-sections and field-interpreted images from the eastern sector are shown in Figures 8 and 9, respectively. In this area, constraints for the upper thrust sheets are scarce, except for the klippes of Keuper and Mendibelza conglomerates carried by the Lakora thrust system on top of the upper Cretaceous (cropping out south of Plateau

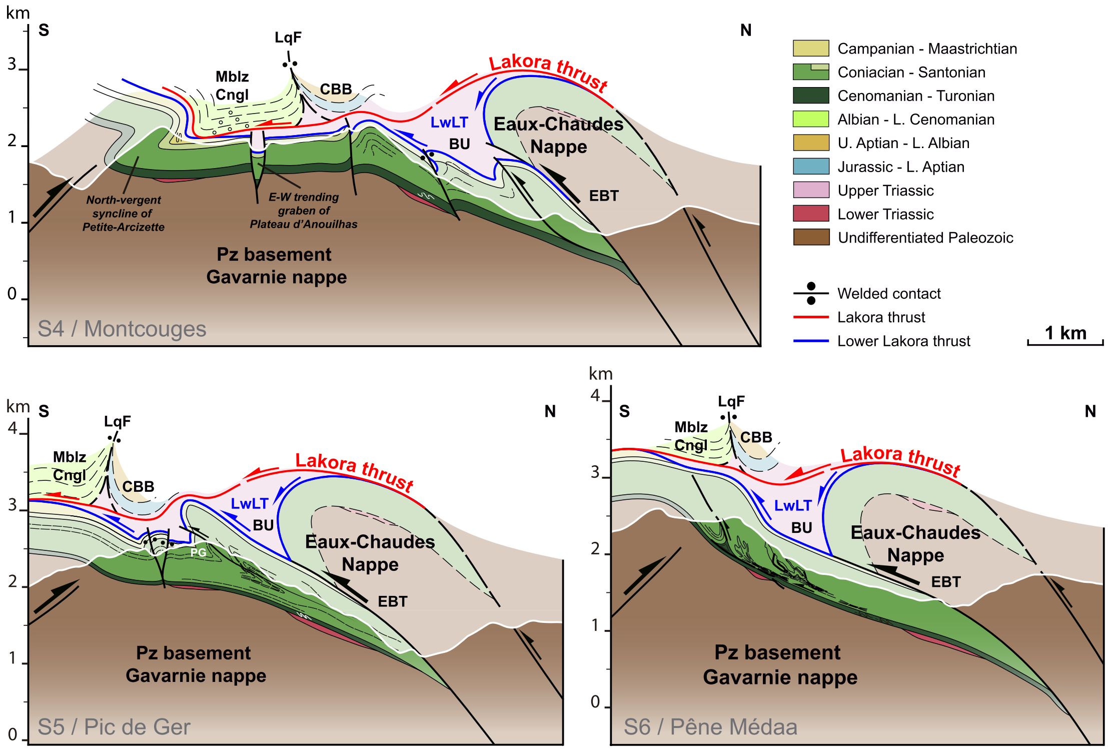

Figure 8. Geological cross-sections of the eastern sector of the Eaux-Chaudes massif featuring the strong ductile deformation in the autochthonous upper Cretaceous. See location in Figure 2. Mblz Cngl, Mendibelza Conglomerates; LqF, Licq Fault; CBB, Chaînons Béarnais Belt; LwLt, Lower Lakora thrust; BU, Bedous Unit (carried by the Lower Lakora thrust); EBT, Eaux-Bonnes Thrust; PG, Pic de Ger in S5. The Eaux-Chaudes fold nappe illustrated in sections in Figure 6 is tentatively interpreted to be replaced in these transects by a simple thrust-related ramp anticline, whereas much of the deformation is transferred to its footwall.

d'Anouilhas, Figure 5 and Sup. 2 for location). Although intensely folded, as reported by Ternet (1965), the upper Cretaceous is broadly in a right-way-up attitude, and in contrast with the western sector, a long-overturned panel is not observed.

The structure equivalent to the allochthonous ECFN is largely eroded, and the continuation of its basal thrust, the Eaux-Bonnes thrust, brings the Devonian on top of the upper Cretaceous in the Valentin valley (Figures 2 and 8). The hanging wall fold structure represented in the sections is speculative and is addressed in the discussion. Paleozoic-bearing thrust sheets (MIN and MVN) are completely eroded over the ECM and are not represented in these sections. The upper Cretaceous of this eastern sector, which is considered as autochthonous to the ECN, is notwithstanding affected by strong ductile deformation (folding, foliation and stretching lineation), in contrast with the western autochthon. Cross-sections S4 to S6 and field images (Figures 8 and 9) illustrate a strain gradient in the autochthonous rocks that increases from west to east. The basal Cretaceous unconformity and the underlying Paleozoic basement are also affected by Alpine ductile deformation, evidenced by a tectonic foliation that can be traced across the unconformity (Figure S6 in Supporting Information S1).

In section S4, from south to north, the first main structure recognized is a north-vergent syncline (Figure 8) in the Paleozoic basement and the overlying upper Cretaceous rocks of the Petite Arcizette peak (Figure 9a; peak location labeled "Pte. Acz." in Figure 5), with intensely folded Campanian flysch rocks in its core (e.g., Dumont et al., 2015). This structure, trending E-W, is rapidly damped to the east. It follows to the north a subhorizontal or north-dipping kilometric-scale panel, cut by steeply dipping normal faults and affected by hectometer-scale south-verging folds (S4 in Figure 8). An asymmetric E-W trending graben in Plateau d'Anouilhas (Figure 5, S4 in Figure 8) preserves Keuper rocks of the Bedous unit, which are allochthonous over the upper Cretaceous. A few hundreds of meters to the west of section S4, two klippes are observed, one carrying the Keuper rocks and the other the Mendibelza conglomerates (Ternet, 1965) (Figures 2, 5, and 8), also interpreted to have been carried by the Lakora thrust system (Figure 4).

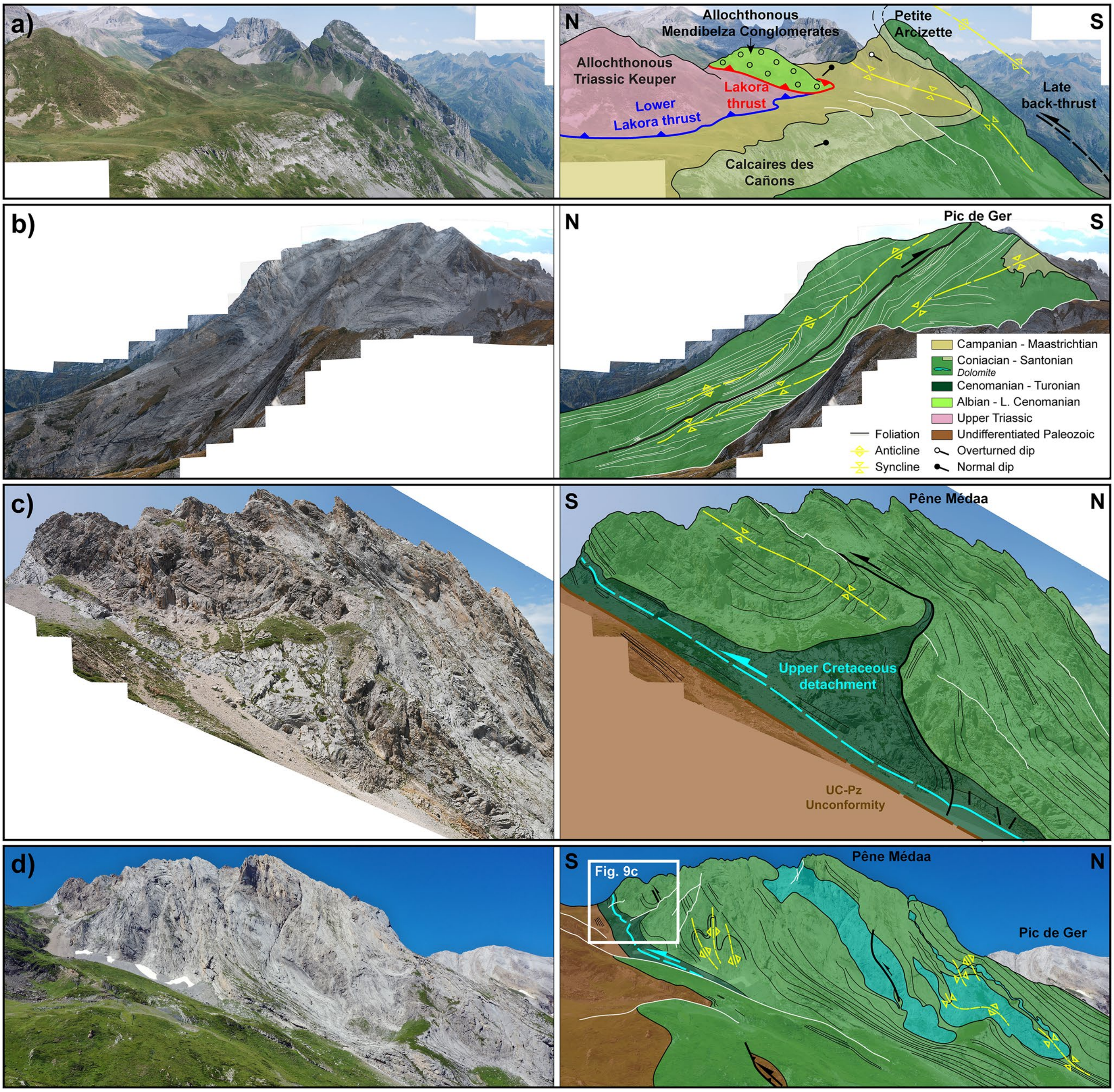

Figure 9. Interpreted panoramas showing different examples of deformation in the upper Cretaceous of the eastern part of the Eaux-Chaudes massif (location of views in Figure 2). (a) View from the west of the Petite Arcizette north-verging syncline. (b) View from the west of the Pic de Ger. A large-scale isoclinal anticline-syncline pair attests for a strong component of ductile deformation in the upper Cretaceous. A view of the syncline on the eastern slope of the Pic de Ger is in Figure 10c. (c) View from the east of the Pêne Médaa showing an intra-Cretaceous detachment at the level of the Cenomanian. Ductile deformation led to folding and squeezing of the lower limestone units above. (d) View from the east of the northern slope of Pêne Médaa showing large-scale dolomitic bodies affected by boudinage, folds and thrusts evidencing intense deformation in this area. Widespread mylonitic foliation in the host limestones is indicated by black lines. Small thrusts affect the basal unconformity.

Further to the east (e.g., S5, Figure 8), folding of the upper Cretaceous becomes more intense in the Pic de Ger fold-thrust fan. Two large-scale south-verging similar folds (the tight anticline-syncline pair shown in Figure 9b), are beautifully exposed on the western slopes of Pic de Ger, and separated by a complex north-dipping thrust fault obliterated by a penetrative schistosity. The axial planes are inclined to the north by ~30° (Figures 8 and 9b). The fold limbs are strongly stretched, the hinges are thickened, and a penetrative axial plane foliation is well-developed.

Secondary internal detachments within the upper Cretaceous are locally observed. The most illustrative examples are represented in section S6 in Figure 8 and in Figures 9c and 9d. The detachment is quite evident by the triangular shape of the Cenomanian limestones which have been ductily squeezed in a thrust footwall (Figure 9c). Asymmetric, tight disharmonic folds are recognized over of the exposed detachment (Figure 9d). Penetrative foliation and stretching lineation are well-developed. Dolostone levels within the dominant limestones appear stretched and boudinaged. Large-scale dolostone boudins are folded and imbricated (Figure 9d) and foliation wraps around these bodies, which occasionally resemble large porphyroclasts.

Several steeply-dipping faults cutting the upper Cretaceous and Paleozoic rocks contain pinched bodies of Keuper and ophites along them, resembling salt welds (e.g., the southern border of Pic de Ger; section S5 in Figure 8). These unusual structures, containing upper Triassic rocks and whose origin is discussed below, were reported by Ternet et al. (2004) and exhibit lateral continuity in W-E direction along the eastern sector of the ECM (Figure 5). Examples are the large ophite body located south of Pic de Breque (Figure 5 for location) and the continuous structure traced from the Montcouges-Pambassibé peaks to the Pic de Ger massif (Figures 2 and 5). On the other hand, to the east of the ECM the unconformity between Paleozoic and Mesozoic rocks is seen affected by small south-verging imbricate thrusts affecting the upper part of the Devonian and the Cenomanian (S6 in Figures 8 and 9d).

5. Discussion

Field observations and the cross-sections of the ECM indicate a complex ductile deformation of the shelf and necking zone of the Iberian margin during the Pyrenean collision. A marked difference in tectonic style is observed between the eastern and western sectors of the massif: the structure of the ECN changes eastwards from a large-scale recumbent fold nappe (the ECFN) to a simple thrust (the Eaux-Bonnes thrust). Deformation is heterogeneously distributed, also from west to east. While the ECFN show high strain localized in the overturned limb, the Pic de Ger fold-thrust fan accommodates strong ductile deformation in the autochthonous Cretaceous succession, and possibly also in the Paleozoic basement (see below). Several factors may have contributed to the complex structure depicted in the cross-sections: (a) the structural inheritance of the Paleozoic basement from the Variscan orogeny, (b) the mechanical stratigraphy of both the Mesozoic and Paleozoic, (c) the geometry and thermal gradient of the Iberian margin due to the mid-Cretaceous hyperextension, and (d) the tectonic burial by the emplacement of the upper thrust sheets. During the inversion of the rifted margin, the structural configuration of the basement and sedimentary cover induced the reactivation of ancient structures and the activation of several detachment levels (Silurian, Keuper and intra-Cenomanian). We focus the discussion on two major key questions: (a) the factors influencing the lateral variation of the ECM structure and (b) the tectonic evolution of the ECFN and overlying thrust units using sequential section restoration.

5.1. What Caused the Structural Contrast Between the Fold Nappe and the Fold-Thrust Domain?

The structural variation of the fold nappe to the fold-thrust system observed in the eastern sector is quite sudden and occurs through a relatively narrow transfer zone near Gourzy (Figures 2, 5, and 6), which coincides with a mechanical contrast in the sub-upper Cretaceous basement.

The Paleozoic basement underlying the ECM is constituted by two clearly differentiated lithological units: the upper Paleozoic metasediments and the Eaux-Chaudes granite pluton (Figures 2, 5, and 6). While the recumbent fold largely concurs with the lateral extent of the granite, the eastern fold-and-thrust fan overlies Devonian rocks (interlayered slates and black limestones), which are mechanically weaker (Figures 2, 5, and 8). The deformation in the Eaux-Chaudes granite is low, whereas the Paleozoic rocks show strong ductile deformation expressed by crenulation and folding superpositions, with a late-phase pervasive folding with southern vergence from minor to large scale. Although the age of the different folding phases (i.e., Variscan vs. Alpine) has not been unequivocally demonstrated, we suggest that the Paleozoic rocks may have experienced superposed shortening from both orogenic cycles (e.g., Sup. 3, showing Alpine foliation crossing the unconformity between the Paleozoic and upper Cretaceous), as also hinted by Ternet (1965).

We postulate that the granite body acted as a forestop, producing a strain shadow zone to the autochthon Mesozoic cover directly overlying it and enabling the transport of the fold nappe originally north of the granite. We must point out that Bresson (1906) already invoked the role of the basement granites for the nucleation of thrust nappes in the study area and Ternet (1965) suggested the importance of the granite in the overall deformation. We thus infer that the Gourzy transfer zone accommodates a structural variation where the structural development of the upper Cretaceous rocks was influenced by the nature of the footwall basement. Similar examples where mechanical stratigraphy and the rheology of basement influenced the structural development of cover were provided for the Alps by Epard (1990), Epard and Escher (1996), and Pfiffner (1993), among others.

The ECFN is bounded by two mechanically weak units, the Silurian black slates at its bottom, and the allochthonous Keuper sheet on the top of the structure, which both acted as lower and upper detachment, respectively. The Silurian detachment allowed a relatively thin upper Paleozoic section to be entrained in the fold core by top-to-the-south shearing as proposed in Figure 6, which in turn enabled the recumbent folding. The Silurian slates, reported as well as the basal detachment of the Gavarnie thrust (Bresson, 1903; Séguret, 1972), have also been proposed to be an effective Alpine detachment eastward of the MVN in the Chiroulet and Lesponne domes (Cochelin et al., 2021). Likewise, we interpret that the upper Paleozoic thrust sheets of the study zone (MIN, MVN, 5MN) are also detached in the Silurian slates.

The allochthonous Bedous Keuper sheet, which probably contained a large proportion of salt, was also key in causing the decoupling of the upper Cretaceous from the overlying thrust sheets. This unit was attributed to the infill of an early Triassic graben later inverted (Labaume & Teixell, 2020; Teixell, 1993), to an olistostrome (Lagabrielle et al., 2010; Stevaux & Zolnai, 1975), or to an extruded salt sheet (García-Senz et al., 2019). We postulate that it was carried by the Lakora thrust system on top of the upper Cretaceous limestones previous to the activation of the Paleozoic-bearing and Eaux-Chaudes nappes. Indeed, the Keuper on the upper Cretaceous limestones was also crucial in enabling recumbent folding of the ECFN as it was expelled from the underlying faulted syncline as attested by few pinched remnants (Caldera et al., 2021; Sup. 1). Hence, the combination of two detachments (the Silurian in the upper Paleozoic and the allochthonous Keuper) with the Eaux-Chaudes granite buttress effect accounts for the intense top-to-the-south shear leading to the development of the Eaux-Chaudes recumbent fold that characterizes the western part of the massif, while a deformable Paleozoic basement and a weak horizon in the lower part of the upper Cretaceous carbonates favored the ductile fold-thrust fan in the eastern part.

5.2. Weld Structures Within the Upper Cretaceous

A singularity of the ECM is the existence of pieces of Keuper shale, ophite and cargneule pinched within the upper Cretaceous limestones. Two main occurrences are recognized: (a) in the tight syncline between the overturned limb of the ECFN and its relative autochthon (Sup. 1), and (b) in steep fault zones cutting the right-way up succession of the eastern upper Cretaceous limestones of the massif (Figures 5 and 6).

A first-order interpretation for the origin of these features can invoke salt tectonics, assimilating the structures that host the Triassic slivers to salt welds. It could be speculated that pre-existing diapirs sourced in Keuper salt originally located under the upper Cretaceous were squeezed during the convergence producing the salt welds. This scenario could be similar to the interpreted salt structures observed in the Jurassic and lower Cretaceous rocks of the CBB (Labaume & Teixell, 2020). However, Keuper rocks are nowhere observed under the upper Cretaceous of the ECM, which always lies unconformable directly over Paleozoic rocks or small Buntsandstein pods. Hence, we consider that the salt welds do not derive from the squeezing of regular diapirs that originally pierced the Cretaceous succession as previously interpreted by Dumont et al. (2015) or Ternet (1965), but rather they must be tertiary welds derived from the squeezing of the allochthonous Keuper sheet of the overlying Lakora unit. Caldera et al. (2021) interpreted in this way the Keuper and ophite slivers in the sheared, isoclinal synform between the fold nappe and its autochthon. During the growth and amplification of the synform, there was an extreme expulsion of the Triassic sheet from the fold core, producing the weld between overturned fold limb and autochthon, and favoring the accumulation of Keuper facies south of the ECFN hinge (Figure 6). Similarly, in the steep welds of the eastern part of the ECM, the Keuper and ophite bodies are observed in the upper part of the upper Creta-

10.1029/2023TC007828

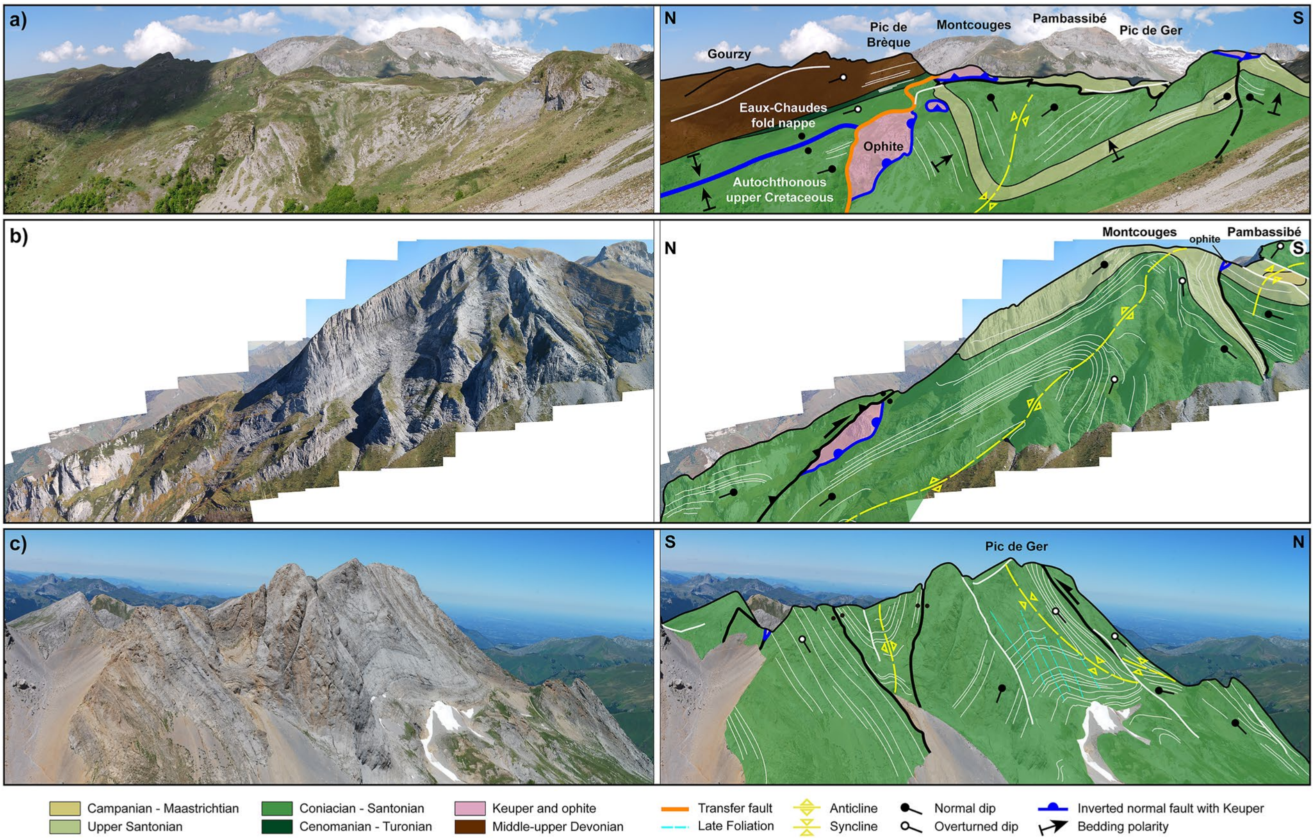

Figure 10. Interpreted panoramas of salt weld-like structures in the eastern Eaux-Chaudes massif (see location of pictures in Figure 2). Weld structures are marked by ophite or Keuper slivers enclosed in the upper Cretaceous limestone and were mapped originally by Ternet (1965), who interpreted them as squeezed diapiric structures coming from below. Here we interpret them as tertiary welds coming from the overlying, allochthonous Keuper sheet (Bedous unit, see text for explanation). (a) View from the west of the Pic de Brèque with the large ophite body in the autochthon of the Eaux-Chaudes fold nappe. The autochthon is deformed by the inversion of a small extensional graben which originally cut the Lower Lakora thrust (see text for explanation). (b) View from the west of the Montcouges and Pambassibé mountains, showing a large, detached anticline limited to the north and south by former extensional faults tectonically inverted. Ophite rocks are pinched in faults, witnessing their compressional tightening. The tightening of the fold is accompanied by foliation in the carbonates. (c) View from the east of the Pic de Ger ridge showing the prominent syncline imaged in Figure 9b and faulted contacts to the south that are marked by Triassic slivers. Strong ductility is evidenced by the penetrative mylonitic foliation which is folded by the syncline. A vertical foliation (blue dashed lines), which is oblique to the axial plane of the fold developed during a later deformation episode.

ceous limestones, associated to high-angle faults (Figure 10) and just below to the Lakora detachment. These faults, that currently may show normal or reverse offsets, are interpreted as former extensional faults synchronous to, or post-dating, the emplacement of the Lakora thrust sheet, as for example, observed in the Anouilhas graben (Figure 5 and Sup. 2), that were subsequently shortened during the deformation of the ECM. The faults often show drag folds on both walls, which can be described as a-type flanking folds according to the classification by Passchier (2001), consistent with early extensional slip. The origin of these extensional faults is unclear, but they may be attributed to flexural load by the overlying thrust sheets to the north (Lakora thrust system and Paleozoic-bearing thrust sheets). Within this context, the ophites and Keuper were down-dropped along the flanking folds associated to the normal faults. Subsequent shortening led to fault steepening, back slip on earlier extensional faults and tightening of the flanking folds, expelling the Keuper and ophites, which were locally pinched forming the observed weld-like structures (Figures 8 and 11). Again, they represent an unusual kind of tertiary salt welds, where the remnants of an allochthonous sheet are not in the contact between the subsalt and suprasalt layers but were entrained between tightly folded subsalt rocks.

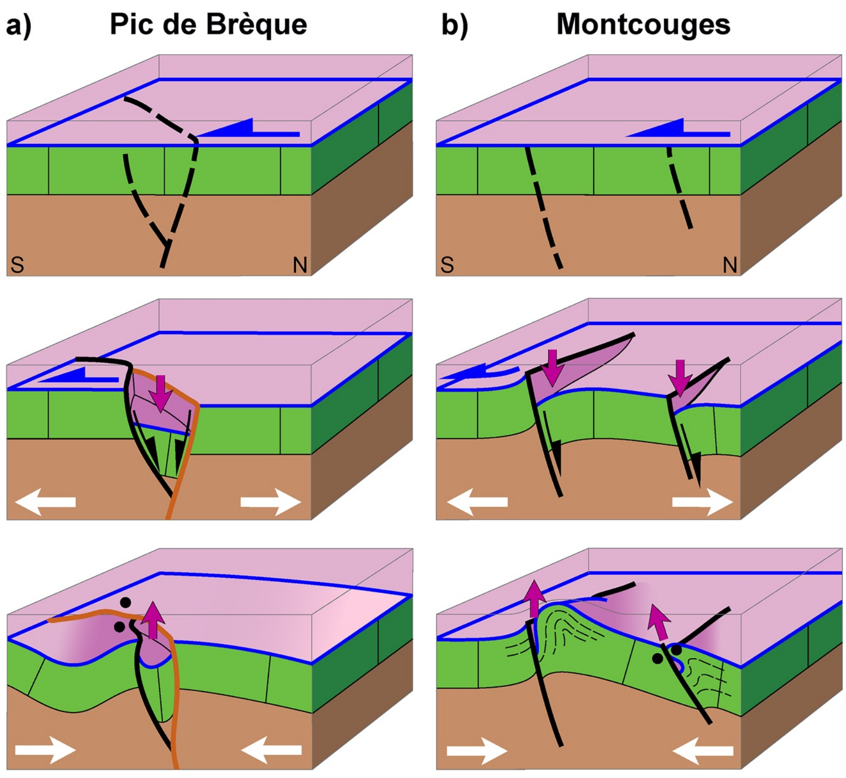

Figure 11. Cartoons explaining the occurrence of pinched Keuper and ophite bodies in the upper Cretaceous carbonates in two sections of the Eaux-Chaudes massif (cf. Figure 5 for location and 10 for illustration). In the first step the Lower Lakora thrust emplaced the allochthon Keuper sheet (Bedous unit) over the upper Cretaceous. In a second step, extensional faulting resulted in the mobilization of the Keuper rocks into depressed areas. Finally, in the shortening stage, structures related with salt were welded when small bodies of upper Triassic were trapped in the core of the previous extensional structures and flattened. The overlying Eaux-Chaudes nappe and subsequent upper nappes are not represented for simplicity. The orange line in (a) corresponds to the Gourzy Transfer Zone.

5.3. Sequential Evolution of the Upper Iberian Margin: Restoration of the Eaux-Chaudes Fold Nappe

Retro-deformation of section S1 (Figure 12) has been performed using bed-lengths and area conservation similar to the methodology followed by Musso Pinatelli et al. (2022) for the Helvetic nappes of the Alps. The Move software was used to account for horizon lengths and cross-sectional areas. The sequential evolution diagram starts at the immediate pre-orogenic stage (mid-Santonian) of the upper Iberian margin.

The reconstruction is based on our field observations and on data compilation from previous works on the west-central Pyrenees, mainly from Labaume and Teixell (2020) and Teixell et al. (2016). Dashed lines in the sketches indicate the trace of the future faults in the next step. Red arrows on the right border of the pictures illustrate the compressional stages while blue arrows indicate the post-orogenic evolution.

The evolution of the ECFN and overlying nappe stack is shown in seven steps, spanning from the mid-Santonian to the present-day (Figure 12).

1. During the mid-Santonian, the uppermost Iberian margin is interpreted as a post-rift shallow-water carbonate shelf (i.e., Calcaires des Cañons), directly covering the Paleozoic basement in the future ECM or the Keuper of the Bedous unit in the future Paleozoic nappes MIN, MVN and 5MN. The boundaries between these units are interpreted as inherited late-Variscan or Mesozoic extensional faults dipping to the north.
   The Bedous unit coincided to the north with the Iberian shelf edge and slope rupture. Northwards, the Mendibelza conglomerates onlap the Paleozoic basement on the necking zone of the margin, limited to the north by a diapiric structure which will be squeezed and become the Licq fault. This limit corresponds to the southern boundary of the CBB, which occupy the former Cretaceous rift axis (Labaume & Teixell, 2020).

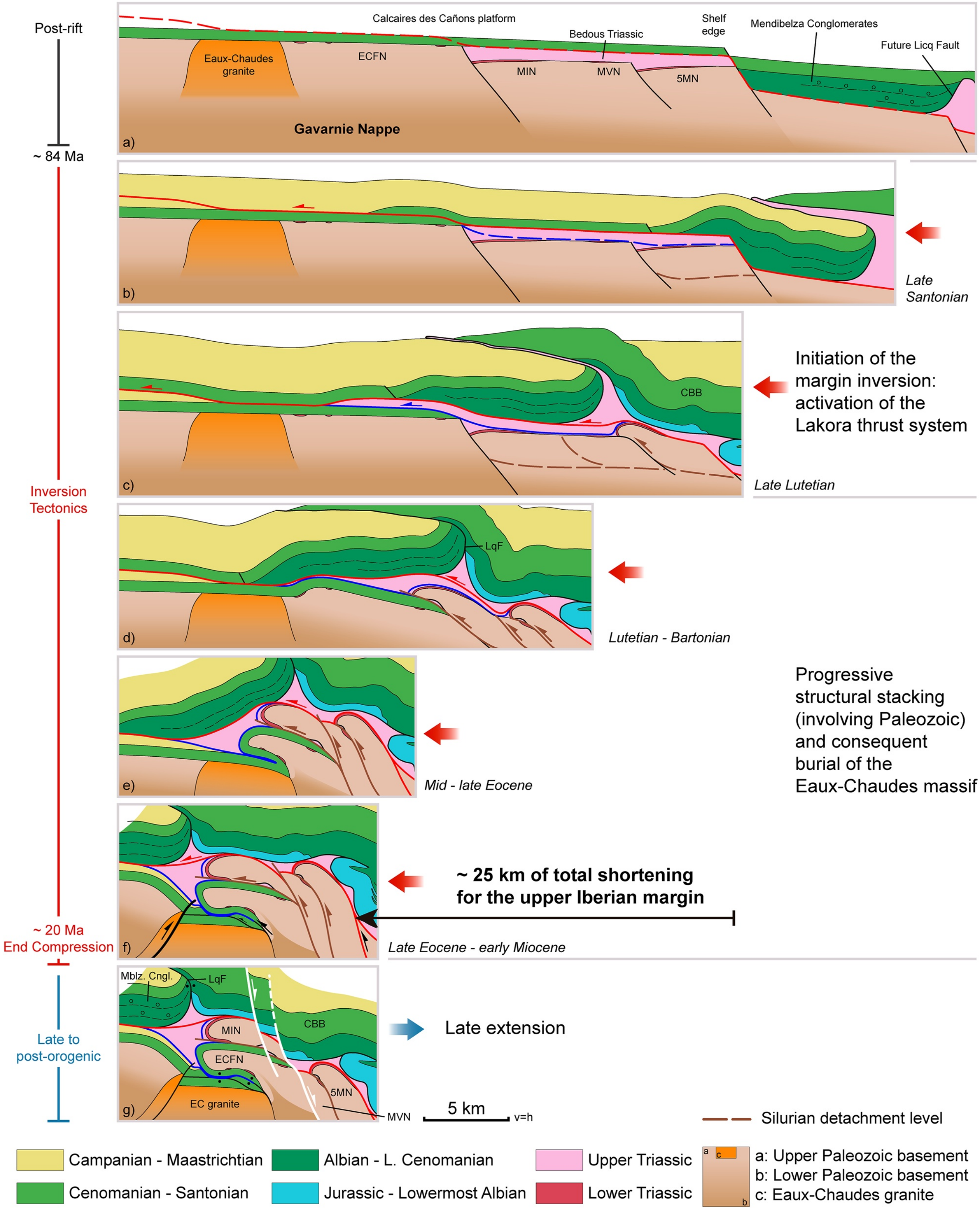
Post-rift
~ 84 Ma
Inversion Tectonics
~ 20 Ma End Compression
Late to post-orogenic
Calcaires des Cañons platform
Bedous Triassic
Shelf edge
Mendibelza Conglomerates
Future Licq Fault
Eaux-Chaudes granite
ECFN
MIN
MVN
5MN
Gavarnie Nappe
a)
b)
Late Santonian
c)
CBB
Initiation of the margin inversion: activation of the Lakora thrust system
Late Lutetian
d)
LqF
Lutetian - Bartonian
e)
Mid - late Eocene
Progressive structural stacking (involving Paleozoic) and consequent burial of the Eaux-Chaudes massif
f)
~ 25 km of total shortening for the upper Iberian margin
Late Eocene - early Miocene
g)
Mblz. Cngl.
LqF
MIN
CBB
ECFN
5MN
EC granite
MVN
Late extension
5 km
v=h
Silurian detachment level
Campanian - Maastrichtian
Cenomanian - Santonian
Albian - L. Cenomanian
Jurassic - Lowermost Albian
Upper Triassic
Lower Triassic
a: Upper Paleozoic basement
b: Lower Paleozoic basement
c: Eaux-Chaudes granite

Figure 12.

2. The early stages of the Pyrenean orogeny were marked by the deepening of the upper Cretaceous shelf due to the flexure of the Iberian margin (e.g., Labaume et al., 2016) and sedimentation of the Campanian-Maastrichtian flysch, the first syn-orogenic unit. The inversion of the basin started with the transport to the south of the salt-detached fold-and-thrust system of the CBB by the thin-skinned Lakora thrust (red line) (Labaume & Teixell, 2020; Teixell et al., 2016). This lasted from the late Santonian until the late Lutetian (Teixell, 1996) or Bartonian stage (e.g., Bosch et al., 2016).
3. Partly contemporaneous with the Lakora *s.s.* thrust, there was the activation of the Lower Lakora thrust (blue line) which emplaced a horse carrying the Bedous evaporitic unit over the future ECM. During or immediately after this stage, the sole detachment on the Silurian of the 5MN (brown line) was active and started to override the southern segment of the Bedous basement.

4, 5. Progressively, the northern Paleozoic thrust sheets (MIN, MVN and 5MN) were emplaced by a propagating basement-involved thin-skinned (Pfiffner, 2017) thrust system, in a piggy-back sequence. The nappe stacking in combination with the Iberian margin flexure and the foredeep sedimentation increased the burial, placing the ECM at a depth of ca. 10 km at Lutetian-Bartonian times (Labaume et al., 2016), and favoring ductile deformation conditions. The ECFN, is interpreted as the last thrust unit to be activated. As the shortening progressed, the Eaux-Chaudes granite faced opposition to deformation, which was localized to the rear. This triggered the nucleation of the antiformal fold to become the ECFN. The fold nappe developed by the hinge migration mechanism as discussed by Guardia et al. (2020).

The hanging wall anticlines of the overlying basement units (MIN and 5MN) were also affected by regional south-directed shearing and turned into recumbent folds. The overturned limbs of the MIN and the 5MN, formed at lower burial than the ECFN, are defined by siliciclastic rocks of the Buntsandstein and display a short (<1 km in 5MN) to moderate length (>2 km in MIN).

The stacking and folding of the Paleozoic units and the ECFN provoked the folding of the Keuper sheet previously emplaced on top. The progressive growth of the overturned limbs and tightening of the synclines resulted in the Keuper expulsion and welding between limbs, as proposed by Caldera et al. (2021).

Based on tectonic-sedimentation relationships in the Jaca foreland basin, it has been proposed that the Lakora and the Eaux-Chaudes nappes remained active up to mid-late Eocene times (Labaume et al., 2016).

6. The southward displacement of the ECFN and Paleozoic-bearing units was followed, since the late Eocene, by the emplacement of the Gavarnie nappe which corresponds to a change in the deformation style. It represents the accretion of a footwall sequence of thick-skinned thrusts favoring the antiformal structure of the Axial Zone (Jolivet et al., 2007; Labaume et al., 2016; Teixell, 1996; Teixell et al., 2016) (Figure 1b). This stage is inferred to correspond to the full crustal collision between the Iberian and European plates which developed from the late Eocene to early Miocene (Teixell et al., 2016). It induced the uplift and arching of the previous structures, which were tilted to the north in the northern limb of the Axial Zone antiform. We interpret that in the ECM, local structural features such as north-verging back-thrusts, back-folds (e.g., Petite Arcizette further east), and sub-vertical foliation were related to this stage.

7. Further uplift of the ECM and adjoining areas by the emplacement of the Guarga thrust to the south (not shown in the figure) are constrained by thermochronology during the latest Eocene-early Miocene (Bosch et al., 2016). Consequently, a large amount of recycled, earlier syn-orogenic deposits and Axial Zone rocks were shed into both the Jaca (Labaume et al., 2016; Puigdefàbregas, 1975; Roigé et al., 2016) and Aquitaine foreland basins (Biteau et al., 2006) (Figure 1a). From the comparison of the present-day and retrodeformed section, we calculate a total shortening of ∼25 km for the entire thrust system.

During late to post-orogenic stages in the Axial Zone, extensional faults cut the whole nappe stack, from the ECFN to the CBB. These faults down-dropped the 5MN and MVN to the north to a lower structural elevation than the MIN and were probably initiated in the final steps of Gavarnie-related arching (Teixell, 1996),

Figure 12. Sketch illustrating the proposed sequence for the compressional inversion of the uppermost Iberian margin in the western Eaux-Chaudes massif, including the structural stacking of the upper thrust units. The granite favored the localization of the deformation into the overturned limb of the recumbent fold and the stacking of multiple northern units by the activation of the upper Paleozoic detachment level (Silurian slates). Red line corresponds to the Lakora thrust carrying the detached CBB and Mendibelza conglomerates. Blue line corresponds to the lower branch of the Lakora thrust carrying the allochthonous Keuper sheet (horse) of the Bedous unit on the Eaux-Chaudes fold nappe (ECFN). Dashed lines show the location of future faults in the following steps. The structure of the pre-inversion stage (a) is modified from the model of hyper-extension of Teixell et al. (2016). The last stage (f) is based on the cross-sections S1 and S2 from Figure 6 for the ECFN, MIN, 5MN and MVN. The kinematic evolution of the CBB is taken from Labaume and Teixell (2020). ECFN, Eaux-Chaudes fold nappe; MIN, Montagnon d'Iseye nappe; 5MN, 5 Monts nappe; MVN, Montagne Verte nappe; CBB, Chaînons Béarnais Belt; Mblz. Cngl, Mendibelza Conglomerates.

and reactivated in Quaternary times by isostatic readjusting induced by erosion (e.g., Dumont et al., 2015; Lacan, 2008; Lacan & Ortuño, 2012).

5.4. Implications on the Collision of the Iberian Margin During the Pyrenean Orogeny

The Alpine Pyrenees in the vicinity of the study area are characterized by two main types of tectonic structures: (a) thick-skinned thrusts (e.g., Gavarnie, Guarga, Broto) detached in depth and enhancing the structural relief along the belt, and (b) thin-skinned thrusts (e.g., Lakora, Larra, Monte Perdido, Cotiella) with shallower detachments in the Mesozoic cover or in the upper Paleozoic (basement short-cuts), and being able to carry sheets over long distances (e.g., Espurt et al., 2019; Teixell et al., 2018). The western Axial Zone, in the hanging wall of the Gavarnie thrust, is usually assumed as weakly deformed in dominant brittle or brittle-ductile conditions during the Alpine orogeny. From our study of the ECM Mesozoic rocks in the Pyrenean hinterland, we conclude that the recumbent fold nappe resulted from "ductile" thin-skinned basement-involved tectonics (nomenclature by Pfiffner, 2017), in an intense simple shear deformation regime associated with detachment in the upper Paleozoic (see Figures 6 and 12). This scenario also prevails for the basement units MIN, MVN and 5MN which are also relatively thin and detached on the Silurian, occasionally featuring recumbent folds on their front. These structures represent the transition between dominant thin-skinned tectonics (i.e., Lakora thrust) to thick-skinned tectonics (i.e., Gavarnie thrust), and were formed in greenschist metamorphic conditions favored by considerable burial. Labaume et al. (2016) proposed ca. 10 km of burial for the ECM during deformation. This is supported by the (U-Th)/He thermochronology of the western Axial Zone (including the ECM), which yielded Miocene cooling ages of reset zircon grains (Bosch et al., 2016). Accounting for that, the thermal reset may have been acquired during the Pyrenean orogeny by a combination of structural stacking and syntectonic sediment burial. Indeed, Curry et al. (2021) recently proposed even larger exhumation (17–19 km) for the whole Axial Zone of the Pyrenees, although these are perhaps too high estimates in view of the paleotemperatures of 300–360°C reported by Caldera et al. (2021) and by Ducoux et al. (2021) in other parts of the northern Axial Zone. The paleotemperatures observed could also be explained by massive fluid flow at the crustal-scale. However, the lack of dense vein networks and hydrothermal alterations in Cretaceous and Paleozoic rocks do not support this hypothesis.

The tectonic style at Eaux-Chaudes has not been reported thus-far in the Alpine Pyrenees, evidencing basement-involved, ductile folding and thrusting. Similar ductile Alpine structures may have been unperceived so-far in other parts of the Paleozoic basement of the Axial Zone. The Eaux-Chaudes deformation structures may be extended ~40 km to the east (cf. Figure 1) conforming the northern wall of the Néouvielle shear zones dated at the early Eocene (circa 50–48 Ma) by radiochronologic methods (Jolivet et al., 2007; Wayne & McCaig, 1998). In the Néouvielle granite, Jolivet et al. (2007) obtained Oligocene to Miocene fission-track cooling ages, similar to the results of Bosch et al. (2016), supporting a deep regional burial, resetting of thermochronometers, followed by a rapid Alpine exhumation. The tilting of the Axial Zone to the west also affects the ECM, covered by the Bedous Triassic sheet and the Iguntze and Mendibelza massifs westwards (cf. Figure 1a). From a regional point of view, the reconciliation with the structure of the Basque massifs is not straightforward due to the tilting and the rapid structural variation related to the influence of transverse structures such as N-S transfer zones (e.g., Saspiturry et al., 2022), similar to what occurs at a smaller scale in the ECM with the Gourzy transfer zone.

6. Conclusions

Six new cross-sections and revised mapping pose the scope of the remarkable along-strike variability within the upper Cretaceous of the ECM of the Pyrenean hinterland. The structure passes from an allochthonous, large-scale recumbent fold core by Paleozoic sediments to the west, into a ductile fold-and-thrust fan in the eastern autochthon, separated by the Gourzy transfer zone. The rheology of the Paleozoic basement underlying the upper Cretaceous is key to this abrupt change in the deformation style. Furthermore, the Eaux-Chaudes granite leads the localization of deformation on top of it, placing the recumbent fold nappe, the eastern upper Paleozoic metasediments (Devonian limestones and schists) allowed spreading of the deformation all over the stratigraphic pile including the upper Cretaceous.

There is no evidence of autochthonous Keuper remnants in between the Paleozoic basement and the upper Cretaceous rocks of the ECM, but an allochthonous Keuper sheet emplaced on the upper Cretaceous by the Lower Lakora thrust in the early stages of the Pyrenean tectonic inversion, facilitated an upper detachment of the structure and the tightening of the recumbent fold. Detachment in Silurian slates was also instrumental in the development of the Eaux-Chaudes tight fold structure, allowing the upper Paleozoic to be entrained in the fold nappe core. Detachment in the Silurian is also inferred for the basement-involved thin thrust sheets that overlie the ECN (Montagnon d'Iseye, Montagne Verte, Cinq Monts).

Unusual tertiary weld-like structures, marked by ophite and claystone/cargneule pinched slivers, attest for the allochthonous Keuper thrust sheet. Unlike common tertiary welds, these are not localized between the subsalt and suprasalt rocks, but within tight synforms or faults of the upper Cretaceous subsalt rocks, from which the bulk of the salt sheet was expelled.

Not only the western ECN conforms to a large recumbent fold evidencing Alpine ductile deformation in this segment of the Pyrenean hinterland, but also the Paleozoic basement units of Cinq Monts and Montagnon d'Iseye show moderately large, overturned limbs delineated by post-Variscan, lower Triassic rocks. The deformation observed is consistent with the paleotemperatures recorded in the post-Paleozoic rocks (300–360°C). The nappe stacking at Eaux-Chaudes and surroundings represents a tectonic style not reported hitherto in the Alpine Pyrenees, evidencing relatively deep burial and/or high inherited thermal gradients during deformation, and basement-involved thin-skinned thrusting. This tectonic style characterizes the inversion of the previous Cretaceous rifted margin during the early stages of the Pyrenean orogeny, at variance to the thick-skinned fan which structured the Axial Zone of the central Pyrenees during the subsequent fully-developed continental collision. It also warns on so-far unperceived Alpine ductile deformation in the basement of the Pyrenean hinterland.

Data Availability Statement

Original data of cleavage and stretching lineation of the upper Cretaceous carbonates generated from this study are openly available in Caldera (2023) on the Mendeley database (https://data.mendeley.com/datasets/2t2rz4khs4/1). *Licence: CC BY 4.0*.

Acknowledgments
This work was supported by the Spanish MINECO/MCIU projects CGL2014-54180 and PGC2018-093903-B-C21. We thank Laura Burrel and Xavier Coll for assistance in the field, and Stéphane Dominguez for helpful discussions in the lab. Petroleum Experts is acknowledged for the academic licenses of the Move software. We also thank J. García-Senz and an anonymous reviewer for comments which helped to improve the manuscript.

References

Aerden, D. G. A. M., & Malavieille, J. (1999). Origin of a large-scale fold nappe in the Montagne Noire, Variscan belt, France. *Journal of Structural Geology*, *21*(10), 1321–1333. https://doi.org/10.1016/S01991-8141(99)00098-X

Alhamawi, M. (1992). Sédimentologie, pétrographie sédimentaire et diagenèse des Calcaires du Crétacé supérieur de la Marge Ibérique (p. 356). Bordeaux 1.

Bastida, F., Aller, J., Fernández, F. J., Lisle, R. J., Bobillo-Ares, N. C., & Menéndez, O. (2014). Recumbent folds: Key structural elements in orogenic belts. *Earth-Science Reviews*, *135*, 162–183. https://doi.org/10.1016/j.earscirev.2014.05.002

Biteau, J.-J., Le Marrec, A., Le Vot, M., & Masset, J.-M. (2006). The Aquitaine Basin. *Petroleum Geosciences*, *12*(3), 247–273. https://doi.org/10.1144/1354-079305-674

Bosch, G., Teixell, A., Jolive, M., Labaume, P., Stockli, D., Domènech, M., & Monié, P. (2016). Timing of Eocene-Miocene thrust activity in the Western Axial Zone and Chaînons Béarnais (west-central Pyrenees) revealed by multi-method thermochronology. *Comptes Rendus Geoscience*, *348*(3–4), 246–256. https://doi.org/10.1016/j.crte.2016.01.001

Bresson, A. (1903). Étude sur les formations anciennes des Hautes et Basses-Pyrénées (Haute-Chaîne). *Bulletin du Service de la Carte Geologique de la France*, *93*(14), 278.

Bresson, A. (1906). Réunion extraordinaire de la Société Géologique de France dans les Pyrénées occidentales en 1906. *Bulletin Societé Géologique France*, *VI*(4), 777–884.

Butler, R. W. H., Tavarnelli, E., & Grasso, M. (2006). Structural inheritance in mountain belts: An Alpine-Apennine perspective. *Journal of Structural Geology*, *28*(11), 1893–1908. https://doi.org/10.1016/j.jsg.2006.09.006

Caldera, N. (2023). Upper Cretaceous cleavage and stretching lineation (Eaux-Chaudes massif) (Version 1) [Dataset]. Mendeley Data. https://doi.org/10.17632/2t2rz4khs4.1

Caldera, N., Teixell, A., Griera, A., Labaume, P., & Lahfid, A. (2021). Recumbent folding in the Upper Cretaceous Eaux-Chaudes massif: A Helvetic-type nappe in the Pyrenees? [Dataset]. Terra Nova, *33*(3), 320–331. https://doi.org/10.1111/ter.12517

Canérot, J., Majesté-Menjoulas, C., & Ternet, Y. (2004). Nouvelle interprétation structurale de la «faille Nord-Pyrénéenne» en vallée d'Aspe (Pyrénées-Atlantiques). Remise en question d'un plutonisme ophitique danien dans le secteur de Bedous. *Comptes Rendus Geoscience*, *336*(2), 135–142. https://doi.org/10.1016/j.crte.2003.11.004

Casteras, M. (1956). Calcaire des Eaux-Chaudes (France, Basses, Pyrénées) – Garumnien – Poudingue de Mendibelza. In *Lexique stratigraphique international* (Vol. 1, 4a VI). Crétacé.

Casteras, M., & Souquet, P. (1964). Sur la constitution et sur la structure de la couverture crétacée de la Zone primaire axiale pyrénéenne à l'Ouest du Pic d'Anie. *Comptes Rendus de l'Académie des Sciences*, *259*(17), 2881–2886.

Chevrot, S., Sylvander, M., Diaz, J., Martin, R., Mouthereau, F., Manatschal, G., et al. (2018). The non-cylindrical crustal architecture of the Pyrenees. *Scientific Reports*, *8*(1), 9591. https://doi.org/10.1038/s41598-018-27889-x

Clerc, C., & Lagabrielle, Y. (2014). Thermal control on the modes of crustal thinning leading to mantle exhumation: Insights from the Cretaceous Pyrenean hot paleomargins. *Tectonics*, *33*(7), 1340–1359. https://doi.org/10.1002/2013TC003471

Clerc, C., Lahfid, A., Monié, P., Lagabrielle, Y., Chopin, C., Poujol, M., et al. (2015). High-temperature metamorphism during extreme thinning of the continental crust: A reappraisal of the North Pyrenean passive paleomargin. *Solid Earth*, *6*(2), 643–668. https://doi.org/10.5194/se-6-643-2015

Cochelin, B., Chardon, D., Denèle, Y., Gumiaux, C., & Le Bayon, B. (2017). Vertical strain partitioning in hot Variscan crust: Syn-convergence escape of the Pyrenees in the Iberian-Armorican syntax. *Bulletin de la Societe Geologique de France*, *188*(6), 39. https://doi.org/10.1051/bsgf/2017026

Cochelin, B., Lemirre, B., Denèle, Y., & de Saint Blanquart, M. (2021). Strain partitioning within bending orogens, new insights from the Variscan belt (Chilouret-Lesponne domes, Pyrenees). *Tectonis*, *40*(7), e2020TC006386. https://doi.org/10.1029/2020TC006386

Conard, M., & Rioult, M. (1977). *Halimeda elliotti* nov. sp., Algue calcaire (chlorophyceae) du Turonien des Alpes-Maritimes (Sud-Est de la France). *Geologie Mediterraneenne*, *4*(2), 43–72.

Corre, B. (2017). La bordure nord de la plaque ibérique à l'Albo-Cénomanien: Architecture d'une marge passive de type ductile (Chaînons Béarnais, Pyrénées Occidentales) (Doctoral dissertation), Rennes 1.

Cruset, D., Vergés, J., Albert, R., Gerdes, A., Benedicto, A., Cantarero, I., & Travé, A. (2020). Quantifying deformation processes in the SE Pyrenees using U-Pb dating of fracture-filling calcites. *Journal of the Geological Society*, *177*(6), 1186–1196. https://doi.org/10.1144/jgs2020-014

Curry, M. E., van der Beek, P., Huismans, R. S., Wolf, S. G., Fillon, C., & Muñoz, J.-A. (2021). Spatio-temporal patterns of Pyrenean exhumation revealed by inverse thermos-kinematic modelling of a large thermochronologic data set. *Geology*, *49*(6), 738–742. https://doi.org/10.1130/G48687.1

Cuvillier, J., Henry, J., Ribis, R., & Villanova, M. (1964). Microfaunes cenomaniennes et santoniennes dans les 'calcaires des canons' (Vallee d'Aspe, Sainte-Engrace, Basses-Pyrenees). *Bulletin de la Societe Geologique de France*, *S7-VI*(2), 273–277. https://doi.org/10.2113/gssgfbull.S7-VI.2.273

Debon, F. (1976). Les Eaux-Chaudes (Pyrénées occidentales): Nouvel exemple de massif granitoïde pyrénéen à structure zonée. *4e RAST, Paris, Societe Geologique de France*, 125.

Debon, F. (1996). Pluton des Eaux-Chaudes. In A. Barnolas & J. C. Chiron (Eds.), *Magmatisme hercynien*, *Synthèse géologique at géophysique des Pyrénées* (Vol. 1, p. 410). BRGM-ITGE.

Debroas, E.-J. (1987). Modèle de basin triangulaire à l'intersection de décrochements divergents pour le fossé albo-cénomanien de la Ballongue (zone nord-pyrénéenne, France). *Bulletin de la Societe Geologique de France*, *III*(5), 887–898. https://doi.org/10.2113/gssgfbull.iii.5.887

Debroas, E.-J. (1990). Le Flysch noir albo-cénomanien témoin de la structuration albienne à sénonienne de la Zone nord-pyrénéenne en Bigorre (Hautes-Pyrénées, France). *Bulletin de la Societe Geologique de France*, *VI*(2), 273–285. https://doi.org/10.2113/gssgfbull.vi.2.273

Delvolvé, J. J. (1987). Un basin synorogénique varisque: le Culm des Pyrénées centro-occidentales (p. 483) (Thèse Doct. Sci.).

Déramond, J., Graham, R., Hossack, H., Baby, J. R., Crouzet, P., & Crouzet, G. (1985). Nouveau modéle de la chaîne des Pyrénées. *Comptes Rendus de l'Académie des Sciences, Paris*, *301*, 1213–1216.

Ducoux, M., Jolivet, L., Masini, E., Augier, R., Lahfid, A., Bernet, M., & Calassou, S. (2021). Distribution and intensity of high-temperature low-pressure metamorphism across the Pyrenean-Cantabrian belt: Constraints on the thermal record of the pre-orogenic hyperextension rifting. *Bulletin de la Societe Geologique de France*, *192*(1), 43. https://doi.org/10.1051/bsgf/2021029

Dumont, T., Replumaz, A., Rouméjon, S., Briais, A., Rigo, A., & Bouillin, J.-P. (2015). Microseismicity of the Béarn range: Reactivation of inversion and collision structures at the northern edge of the Iberian plate. *Tectonics*, *34*(5), 934–950. https://doi.org/10.1002/2014TC003816

Epard, J.-L. (1990). La nappe de Morcles au sud-ouest du Mont-Blanc. Stratigraphie (Thèse de doctorat). Université de Lausanne.

Epard, J.-L., & Escher, A. (1996). Transition from basement to cover: A geometric model. *Journal of Structural Geology*, *18*(5), 533–548. https://doi.org/10.1016/S0191-8141(96)80022-8

Espurt, N., Angrand, P., Teixell, A., Labaume, P., Ford, M., de Saint Blanquart, M., & Chevrot, S. (2019). Crustal-scale balanced cross-section and restoration of the Central Pyrenean belt (Nestes-Cinca transect): Highlighting the structural control of Variscan belt and Permian-Mesozoic rift systems on mountains building. *Tectonophysics*, *764*, 25–45. https://doi.org/10.1016/j.tecto.2019.04.026

Floquet, M., Mathey, B., Rosse, P., & Vadot, J. P. (1988). Age cenomanien et turono-coniacien des calcaires de Sare (Pays Basque, France-Espagne); consequences paleomorphologiques et tectogenetiques pour les Pyrenees occidentales. *Bulletin de la Societe Geologique de France*, *IV*(6), 1021–1027. https://doi.org/10.2113/gssgfbull.IV.6.1021

Ford, M., Masini, E., Vergés, J., Pik, R., Ternois, S., Léger, J., et al. (2022). Evolution of a low convergence collisional orogen: A review of Pyrenean orogenesis. *Bulletin de la Societe Geologique de France*, *193*(1), 19. https://doi.org/10.1051/bsgf/2022018

Fournier, E. (1905). Etudes géologiques sur la partie occidentale de la chaîne des Pyrénées, entre la vallée d'Aspe et celle de la Nieve. *Bulletin de la Société Géologique de la France*, *5*, 699–723.

García-Sansegundo, J., Poblet, J., Alonso, J. L., & Clariana, P. (2011). Hinterland-foreland zonation of the Variscan orogen in the Central Pyrenees: Comparison with the northern part of the Iberian Variscan massif. *Geological Society, London, Special Publications*, *349*(1), 169–184. https://doi.org/10.1144/sp349.9

García-Senz, J., Pedrera, A., Ayala, C., Ruiz-Constán, A., Robador, A., & Rodríguez-Fernández, L. R. (2019). Inversion of the north Iberian hyperextended margin: The role of exhumed mantle indentation during continental collision. In J. A. Hammerstein (Ed.), *Fold and thrust belts: Structural style, evolution and exploration* (p. 490). Geol. Soc., Spec. Publ. https://doi.org/10.1144/SP490-2019-112

Golberg, J. M. (1987). Le métamorphisme mésozoique dans la partie orientale des Pyrénées: Relations avec l'évolution de la chaîne au Crétacé. *Documents et Travaux - Centre Geologique et Geophysique de Montpellier*, *14*, 235.

Golberg, J. M., & Leyreloup, A. F. (1990). High temperature-low pressure Cretaceous metamorphism related to crustal thinning (Eastern North Pyrenean Zone, France). *Contributions to Mineralogy and Petrology*, *104*(2), 194–207. https://doi.org/10.1007/BF00306443

Grool, A. R., Ford, M., Vergés, J., Huismans, R. S., Christophoul, F., & Dielforder, A. (2018). Insights into the crustal-scale dynamics of a doubly vergente orogen from a quantitative analysis of its forelands: A case study of the Eastern Pyrenees. *Tectonics*, *37*(2), 450–476. https://doi.org/10.1002/2017TC004731

Guardia, M., Griera, A., Kaus, B., Piccolo, A., & Teixelll, A. (2020). Mechanical controls on recumbent folding from 2D numerical simulations. Applications to the Eaux-Chaudes fold nappe (west-central Pyrenees). In *EGU general assembly 2020, online, 4–8 May 2020*. EGU2020-13505. https://doi.org/10.5194/egusphere-egu2020-13505

Guerrot, C. (2001). Datation du pluton des Eaux-Chaudes. In Y. Ternet, C. Majesté-Menjoulas, J. Canérot, T. Baudin, A. Cocherie, C. Guerrot, et al. (Eds.), *(2004). Notice explicative, Carte géol. France (1/50.000), feuille Laruns-Somport (1069)* (pp. 185–187). BRGM.

Izquierdo-Llavall, E., Román-Berdiel, T., Casas, A. M., Oliva-Urcia, B., Gil-Peña, I., Soto, R., & Jabaloy, A. (2012). Magnetic and structural study of the Eaux-Chaudes instrusion: Understanding the Variscan deformation in the Western Axial Zone (Pyrenees). *International Journal of Earth Sciences*, *101*(7), 1817–1834. https://doi.org/10.1007/s00531-012-0760-9

Jackson, M., & Hudec, M. (2017). *Salt tectonics: Principles and practice*. Cambridge University Press. https://doi.org/10.1017/9781139003988

Jammes, S., Manatschal, G., Lavier, L., & Masini, E. (2009). Tectonosedimentary evolution related to extreme crustal thinning ahead of a propagating ocean: Example of the western Pyrenees. *Tectonics*, *28*(4), 1–24. https://doi.org/10.1029/2008TC002406

Jolivet, M., Labaume, P., Monié, P., Brunel, M., Arnaud, N., & Campani, M. (2007). Thermochronology constraints for the propagation sequence of the south Pyrenean basement thrust system (France-Spain). *Tectonics*, *26*(5), 1–17. https://doi.org/10.1029/2006TC002080

Labaume, P., Meresse, F., Jolivet, M., Teixell, A., & Lahfid, A. (2016). Tectonothermal history of an exhumed thrust-sheet-top basin: An example from the south Pyrenean thrust belt. *Tectonics*, *35*(5), 1280–1313. https://doi.org/10.1002/2016TC004192

Labaume, P., & Teixell, A. (2020). Evolution of salt structures of the Pyrenean rift (Chaînons Béarnais, France): From hyper-extension to tectonic inversion [Dataset]. Tectonophysics, *785*, 228451. https://doi.org/10.1016/j.tecto.2020.228451

Lacan, P. (2008). Activité Sismotectonique Plio-Quaternaire de l'Ouest des Pyrénées (Ph.D. Thesis). Université de Pau et des Pays de l'Adour.

Lacan, P., & Ortuño, M. (2012). Active tectonics of the Pyrenees: A review. *Journal of Iberian Geology*, *38*(1), 9–30. https://doi.org/10.5209/rev_JIGE.2012.v38.n1.39203

Lagabrielle, Y., & Bodinier, J. L. (2008). Submarine reworking of exhumed subcontinental mantle rocks: Field evidence from the Lherz peridotites, French Pyrenees. *Terra Nova*, *20*(1), 11–21. https://doi.org/10.1111/j.1365-3121.2007.00781.x

Lagabrielle, Y., Labaume, P., & de Saint Blanquat, M. (2010). Mantle exhumation, crustal denudation, and gravity tectonics during Cretaceous rifting in the Pyrenean realm (SW Europe): Insights from the geological setting of the lherzolite bodies. *Tectonics*, *29*, 1–26. https://doi.org/10.1029/2009TC002588

Majesté-Menjoulas, C. (1968). Le Peléozoïque au Nord du synclinorium des Eaux-Chaudes (Pyrénées Atlantiques) (Thèse Doct. 3[e] cycle).

Manatschal, G., Chenin, P., Lescoutre, R., Miró, J., Cadenas, P., Saspiturry, N., et al. (2021). The role of inheritance in forming rifts and rifted margins and buildings collisional orogens: A Biscay-Pyrenean perspective. *Bulletin de la Societe Geologique de France*, *192*(1), 55. https://doi.org/10.1051/bsgf/2021042

Masini, E., Manatschal, G., Tugend, J., Mohn, G., & Flament, J.-M. (2014). The tectono-sedimentary evolution of a hyper-extended rift basin: The example of the Arzacq-Mauléon rift system (Western Pyrenees, SW France). *International Journal of Earth Sciences*, *103*(6), 1569–1596. https://doi.org/10.1007/s00531-014-1023-8

Matte, P. (2002). Les plis hercyniens kilométriques couchés vers l'ouest-sudouest dans la région du pic du Midi d'Ossau-col du Somport (zone axiale des Pyrénées occidentales). *Comptes Rendus Geoscience*, *334*(10), 773–779. https://doi.org/10.1016/s1631-0713(02)01808-4

Mirouse, R. (1962). Recherches géologiques dans la partie occidentale de la zone primaire axiale des Pyrénées (p. 451) (Thèse État, Toulousse). Mém. Serv. Carte géol. Fr. (1966).

Mouthereau, F., Filleaudeau, P.-Y., Vacherat, A., Pik, R., Lacombe, O., Fellin, M. G., et al. (2014). Placing limits to shortening evolution in the Pyrenees: Role of margin architecture and implications for the Iberia/Europe convergence. *Tectonics*, *33*(12), 2283–2314. https://doi.org/10.1002/2014TC003663

Muñoz, J. A. (1992). Evolution of a continental collision belt: ECORS-Pyrenees crustal balanced cross-section. In K. McClay (Ed.), *Thrust tectonics* (pp. 235–246). Springer. https://doi.org/10.1007/978-94-011-3066-0_21

Musso Pinatelli, F., Mair, D., Berger, A., Schlunegger, F., Wiederkehr, M., Kurmann, E., et al. (2022). 4D reconstruction of the Doldenhorn nappe-basement system in the Aar massif: Insights into late-stage continent-continent collision in the Swiss Alps. *Tectonophysics*, *843*, 229586. https://doi.org/10.1016/j.tecto.2022.229586

Ortí, F., Pérez-López, A., & Salvany, J. M. (2017). Triassic evaporites of Iberia: Sedimentological and palaeogeographical implications for the western Neotethys evolution during the Middle Triassic-Earliest Jurassic. *Palaeogeography, Palaeoclimatology, Palaeoecology*, *471*, 157–180. https://doi.org/10.1016/j.palaeo.2017.01.025

Passchier, C. W. (2001). Flanking structures. *Journal of Structural Geology*, *23*(6–7), 951–962. https://doi.org/10.1016/S0191-8141(00)00166-8

Pfiffner, O. A. (1993). The structure of the Helvetic nappes and its relation to the mechanical stratigraphy. *Journal of Structural Geology*, *15*(3–5), 511–521. https://doi.org/10.1016/0191-8141(93)90145-Z

Pfiffner, O. A. (2017). Thick-skinned and thin-skinned tectonics: A global perspective. *Geosciences*, *7*(3), 71. https://doi.org/10.3390/geosciences7030071

Puigdefàbregas, C. (1975). La sedimentación molásica en la cuenca de Jaca. *Pirineos*, *104*, 1–188.

Puigdefàbregas, C., & Souquet, P. (1986). Tecto-sedimentary cycles and depositional sequences of the Mesozoic and Tertiary from the Pyrenees. *Tectonophysics*, *129*(1–4), 173–203. https://doi.org/10.1016/0040-1951(86)90251-9

Razin, P. (1989). Evolution tecto-sédimentaire alpine des Pyrénées Basques à l'Ouest de la transformante de Pamplona (province du Labourd) (Thèse Doctorat) (p. 464). Université de Bordeaux III.

Roigé, M., Gómez-Gras, D., Remacha, E., Daza, R., & Boya, S. (2016). Tectonic control on sediment sources in the Jaca basin (Middle and Upper Eocene of the South-Central Pyrenees). *Comptes Rendus Geoscience*, *348*(3–4), 236–245. https://doi.org/10.1016/j.crte.2015.10.005

Saspiturry, N., Allanic, C., Serrano, O., Courrioux, G., Baudin, T., Le Bayon, B., et al. (2022). Upper lithospheric transfer zones driving the non-cylindricity of the West-Pyrenean orogenic prism (Mauléon hyperextended basin). *Journal of Structural Geology*, *156*, 104535. https://doi.org/10.1016/j.jsg.2022.104535

Séguret, M. (1972). *Étude tectonique des nappes et séries décollées de la partie centrale du versant sud des Pyrénées*. In *Sér. Géol. Struct*. (Vol. 2). Publications de l'Univ. des Sciences et Techniques du Languedoc.

Soto, J. I., Flinch, J. F., & Tari, G. (2017). *Permo-Triassic Salt Provinces of Europe, North Africa and the Atlantic margins: Tectonics and hydrocarbon potential*. Elsevier. Print.

Souquet, P. (1967). Le Crétacé supérieur sud-pyrénéen en Catalogne, Aragon et Navarre (Thèse Doct. Sci.). Univ. Toulousse.

Souquet, P., Debroas, É. J., Boirie, J. M., Pons, P., Fixari, G., Roux, J. C., et al. (1985). Le Groupe du Flysch noir (Albo-Cénomanien) dans les Pyrénées. *Bulletin – Centres de Recherches Exploration-Production Elf- Aquitaine*, *9*(1), 183–252.

Stevaux, J., & Winnock, E. (1974). Les bassins du Trias et du Lias inférieur d'Aquitaine et leurs épisodes évaporitiques. *Bulletin de la Societé Géologique de France*, *S7-16*(6), 679–695. https://doi.org/10.2113/gssgfbull.S7-XVI.6.679

Stevaux, J., & Zolnai, G. (1975). *Les Olistostromes du Sud de l'Aquitaine dans la dynamique du Bassin*. IXe Congrès International de Sédimentologie.

Teixell, A. (1993). Coupe géologique du massif d'Igountze: Implications sur l'évolution structurale de la bordure sud de la Zone nord-pyrénéenne occidentale. *Comptes Rendus de l'Académie des Sciences, Paris*, *316*, 1789–1796.

Teixell, A. (1996). The Ansó transect of the southern Pyrenees: Basement and cover thrust geometries. *Journal of the Geological Society of London*, *153*(2), 301–310. https://doi.org/10.1144/gsjgs.153.2.0301

Teixell, A., Durney, D. W., & Arboleya, M. L. (2000). Stress and fluid control on décollement within competent limestone. *Journal of Structural Geology*, *22*(3), 349–371. https://doi.org/10.1016/S0191-8141(99)00159-5

Teixell, A., Labaume, P., Ayarza, P., Espurt, N., de Saint Blanquart, M., & Lagabrielle, Y. (2018). Crustal structure and evolution of the Pyrenean-Cantabrian belt: A review and new interpretations from recent concepts and data. *Tectonophysics*, *724–725*, 149–170. https://doi.org/10.1016/j.tecto.2018.01.009

Teixell, A., Labaume, P., & Lagabrielle, Y. (2016). The crustal evolution of the west-central Pyrenees revisited: Inferences from a new kinematic scenario [Dataset]. Comptes Rendus Geoscience, *348*(3–4), 257–267. https://doi.org/10.1016/j.crte.2015.10.010

Ternet, Y. (1965). Étude du synclinal complexe des Eaux-Chaudes (Basses-Pyrénées) (Thèse Doctorat 3º Cycle) [Dataset]. Faculté des Sciences de l'Université de Toulouse, 332.

Ternet, Y., Majesté-Menjoulas, C., Canérot, J., Baudin, T., Cocherie, A., Guerrot, C., & Rossi, P. (2004). Carte géologique de la France: Laruns-Somport [Dataset]. Bureau de Recherches Géologiques et Minières, scale 1:50.000, feuille nº1069. Retrieved from http://ficheinfoterre.brgm.fr/Notices/1069N.pdf

Tugend, J., Manatschal, G., Kusznir, N. J., Masini, E., Mohn, G., & Thinon, L. (2014). Formation and deformation of hyperextended rift Systems: Insights from rift domain mapping in the Bay of Biscay-Pyrenees. *Tectonics*, *33*(7), 1239–1276. https://doi.org/10.1002/2014TC003529

Wayne, D. M., & McCaig, A. M. (1998). Dating fluid-flow in shear zones: Rb-Sr and U-Pb studies of syntectonic veins in Néouvielle Massif, Pyrenees. In J. Parnell (Ed.), *Dating and duration of fluid flow and fluid-rock interactions* (Vol. 144, pp. 129–135). The Geological Society of London. (Special Publications). https://doi.org/10.1144/GSL.SP.1998.144.01.09